1-1-2021

REMOVAL OF HEAVY METALS FROM WATER USING NATURAL BAUXITE

Hashindra Kumari Herath
University of Mississippi

REMOVAL OF HEAVY METALS FROM WATER USING NATURAL BAUXITE

A thesis

presented in partial fulfillment of requirements

for the degree of Master of Science

in the Department of Geology and Geological Engineering

The University of Mississippi

by

HASHINDRA K HERATH

December 2021

ABSTRACT

Bauxite, the principal ore of aluminum is a potential low-cost sorbent to treat heavy metal-contaminated water. This work studied the ability of raw bauxite to adsorb Pb^{2+}, Cu^{2+}, Ni^{2+}, and Co^{2+} ions in natural waters and the dependency of the sorption efficiency on the initial metal ion concentration in water, contact time, the 'type' of bauxite, and the effect of coexisting metals. Goethite-rich (B1) and kaolinite-rich (B2) bauxites were sampled in Pontotoc County, Mississippi. Single element and multi-element (ME) solutions were prepared by introducing the metals at concentrations of 10, 100, and 500 ppb in lake water. The solutions were left in contact with 0.25 g of prepared bauxite powder over contact periods of 3, 6, 12, 24, and 48 hours without changing other physicochemical parameters. The filtrates were analyzed using Inductively Coupled Plasma-Mass Spectrometer (ICP-MS). Bauxite mineralogy was examined using X-ray Diffraction (XRD) and Scanning Electron Microscope with Energy Dispersive X-ray spectroscopy (SEM-EDS).

Except in certain Ni^{2+}-containing systems, bauxite could remove metals from the water. Overall, the percent sorption tends to decrease with increase in initial metal concentration of the metals tested. Some systems particularly Pb^{2+}- and Cu^{2+}-containing recorded the highest percent sorption (>90%) at 100 ppb but it dropped (around 20-40%) at 500 ppb. Metal uptake generally increases with increase in initial metal concentration but the increment between the 100 ppb and the 500 ppb systems is often less pronounced. The sorption by B1 is relatively more dependent on the initial metal concentration. Overall, the removal efficiency of B2 is slightly higher. A

clear dependency of sorption on contact time was not observed. Bauxite is selective towards Cu^{2+} and Pb^{2+} but the near-complete removal of Cu^{2+} in some systems suggests that Cu^{2+} is favored. Co^{2+} and Ni^{2+} seem to have similar affinities toward bauxite, but Ni^{2+} showed negative percent sorption values at certain longer contact times and higher concentrations. The removal efficiencies of both bauxites decreased in the ME-experiments. Adsorption is possibly Langmuir-type, suggesting chemisorptive monolayer formation. Fe-Al Oxyhydroxide and clay surfaces are the possible adsorption sites in bauxite that bind metals via specific adsorption and ion exchange.

DEDICATION

I am forever grateful for the unconditional, unequivocal love and support I receive from my parents, and my brother, Ishika. I dedicate all my accomplishments and success to you, including this.

LIST OF ABBREVIATIONS

XRD	X-ray diffraction
UM	University of Mississippi
SEM-EDS	Scanning electron microscope with energy dispersive X-ray spectroscopy
ME	Multi-element
B1	Bauxite sample 1
B2	Bauxite sample 2
ICPMS	Inductively coupled plasma-mass spectrometer
CEC	Cation exchange capacity

ACKNOWLEDGEMENTS

I would like to express my sincere gratitude to my advisor Dr. Inoka Widanagamage for taking me as her student and giving me the opportunity to carry out this project. Thank you so much for your ever encouraging and motivating guidance. I am extremely grateful to Dr. Brian Platt, for serving in my advising committee and his contribution to this work. I really appreciate your assistance during field work, and especially the constructive feedback and helpful tips you provided to improve my writing skills. I would also like to extend my gratitude to Drs. Andrew O'Reilly and James Cizdziel for serving in my thesis committee and providing invaluable feedback on my work. Your thoughtful, detailed comments and suggestions are respectfully acknowledged. Dr. Cizdziel also let me use his lab at the Department of Chemistry and Biochemistry for some of the analyses. Many thanks to him and Byunggwon Jeon for especially helping me with the process of ICP-MS analysis.

I would like to recognize the assistance I received from Michael Gratzer, Timothy Clark, and Pamela Akakpo during field sampling and/or lab work. Your company and support will always be remembered. I am grateful to Dr. Vijayasankar Raman at the National Center for Natural Products Research, School of Pharmacy for guiding and helping me in conducting the SEM analysis. I acknowledge the generous financial support from the Gulf Coast Association of Geological Societies and the Robert Woolsey Memorial Research Scholarship that helped with

the cost of laboratory analyses. I am so thankful to the Department of Geology and Geological Engineering for all the knowledge, support, and the opportunities for me to grow professionally. I extend my thanks to all my fellow graduate students for their continuous encouragement and friendship.

TABLE OF CONTENTS

LIST OF TABLES

LIST OF FIGURES

CHAPTER 1 - INTRODUCTION

Heavy metals (e.g., Cu, Ni, Pb, and Cr) are toxic and have direct adverse effects on humans and animals (Ageena, 2010). They have short term (acute toxicity) and long term (e.g., carcinogenicity) adverse effects on humans and animals (Bereket et al., 1997; Ageena, 2010; Genç-Fuhrman et al., 2007). These inorganic pollutants are persistent, accumulative, and not bio-degradable (Genç-Fuhrman et al., 2007; Jiang et al., 2010; Rao & Kashifuddin, 2014), thus the toxicity tends to increase through biomagnification further up the food chains. These metals can be dispersed beyond their sources through natural weathering and transport processes (Fuge et al., 1993). Industries such as electric appliances manufacturing, pigment, cosmetics, electroplating, mining, metallurgical engineering, smelting, and dyeing produce various contaminants including heavy metals in wastewater effluents. Agricultural pollutants such as pesticides and fertilizers can contribute to metal contamination in water and soil as well (Halim et al., 2003; Ali & Gupta, 2007; Hedrich & Johnson 2014; Uddin, 2017). Urban stormwater runoff (road runoff) is also rich in heavy metals due to the input from building materials and traffic-related sources such as brake linings and tire wear (Genç-Fuhrman et al., 2007).

Sorption processes affect the fate of metal ions in sediment-water-soil environments (Atasoy & Bilgic, 2018). Their mobility and bioavailability are controlled by the extent to which they sorb onto the solid phases (Singh et al., 2001). Clay-size particles, silicate clay interlayers, organic matter, and metal (e.g., Fe-Al) oxides are potential sites for metal sorption due to their high surface area and high capacities for scavenging metal ions in solution (Bargar et al., 1997b;

Atasoy & Bilgic, 2018). Speciation of metal ions between solid and aqueous phases is controlled by factors such as the ionic strength, pH, the concentration of the complexing ions, and the surface area and surface charge of the substrate (Petrović et al., 1999).

In order to regulate the discharge of these contaminants to natural aquatic systems and to treat polluted water/soil, several treatment technologies have been proposed/practiced. Chemical precipitation, reverse osmosis, coagulation-flocculation, ion exchange, membrane filtration processes, biological treatments, electrolysis, and adsorption are some of the techniques that have been developed over time to remove these metal ions from wastewaters and soil (Genç et al., 2003; Adebowale et al., 2005; Aziz et al., 2008; Saadi et al., 2013). Most of these techniques have disadvantages such as high cost, higher energy and space consumption, low efficiency at specific conditions, and toxic waste production (Saadi et al., 2013). For example, reverse osmosis, an effective treatment method can be very costly due to the need of frequent replacement of membranes. Ion exchange is a sophisticated and expensive technique (Jiang et al., 2010). Methods such as solvent extraction and electrolytic processes are considered to be cost-effective for more concentrated systems only (Bhattacharyya & Gupta, 2008a). Similarly, processes like chemical precipitation are not suitable to remove metals at low concentrations, and also, they produce a large amount of sludge (Jiang et al., 2010). Adsorption appears to be one of the most widely used techniques to remove heavy metals from aqueous solutions due to benefits such as availability, low cost, profitability, efficiency, effectiveness, and ease of operation compared to other techniques (Rao et al., 2014; Uddin, 2017; Lehmann et al., 1999; Yabe & Oliveira, 2003; Ghosh & Bhattacharyya, 2002). The process is simple where a substance is separated from one phase and accumulated at another surface (Weber, 1985).

Various sorbents such as goethite (Forbes et al., 1976), kaolinite (Jiang et al., 2010), sulfate and phosphate modified kaolin (Adebowale et al., 2005), granular activated carbon (Loganathan et al., 2018), limestone (Aziz et al., 2008), fly ash, bauxol-coated sand, zeolite, iron oxide-coated sand (Genç-Fuhrman et al., 2007), and γ-alumina (Saadi et al., 2013) have been used in studies developed on removing heavy metals (e.g., Pb, Cu, Zn, Co, Cd) from water. The selection of the substrate usually depends on factors such as the concentration of metal ions in solution, sorption capacity of the sorbent, and efficiency/cost ratio. Natural sorbents are generally preferred over synthetic material due to low cost and availability, and sorbents like peat and varieties of clays are much favored over substances like zeolite and activated carbon especially when cost limitations play a critical role in implementing a developed method (Adebowale et al., 2005; Ghosh & Mishra, 2017).

Bauxite is a naturally occurring, heterogeneous material mainly composed of aluminum hydroxide minerals (Alshaebi et al., 2009). The major Al-hydroxide minerals typically found in bauxite are gibbsite ($Al(OH)_3$), boehmite (AlO(OH)), and diaspore (α-AlO(OH)). In addition to Al-hydroxides, silica, iron oxides, titania, aluminum silicates are often present in bauxite along with other impurities (Alshaebi et al., 2009; Atasoy & Bilgic, 2018). Owing to its heterogeneity, bauxite does not have a fixed chemical or mineralogical composition. Different bauxites could have different compositions due to differences in formation processes, climatic conditions, and parent material (Malakootian et al., 2014). Therefore, the term bauxite is often used to describe a range of materials that could possibly have different physical, compositional, and genetic characteristics. Due to the high abundance of Al-Hydroxide minerals, the bulk of global bauxite production is used to produce alumina (Al_2O_3) through Bayer process, which is a wet chemical caustic leach process performed under heat and pressure (Brunori et al., 2005; Alshaebi et al.,

2009). Therefore, bauxite is considered the principal ore of Al. Bauxite can be proposed as a low-cost sorbent for heavy metal removal from aqueous solutions due to factors such as availability, high surface area, and effective adsorption capacity. Several studies have introduced bauxite as an effective sorbent in removing inorganic substances particularly metal(loid) oxianions such as Cr(VI) and As(V), and anions such as F^- and $(PO_4)^{3-}$ (Alshaebi et al., 2009; Lavecchia et al., 2012; Cherukumilli et al., 2017) but, raw bauxite has not been widely applied in treating water polluted with (divalent) heavy metal cations.

However, bauxite residue/bauxite tailings/red mud (from alumina production) has been commonly used in studies for that purpose (López et al., 1998; Apak et al., 1998; Wang et al., 2008). Bauxite or red mud is often modified/processed (e.g., calcination, thermal activation, acid activation) when used in treating water contaminated with those pollutants (Altundoğan et al., 2002; Genç-Fuhrman et al., 2004; Das et al., 2005; Baral et al., 2007). Acids such as H_2SO_4, HNO_3, and HCl are typically used in acid treatments (Cengeloglu et al., 2006; Huang et al., 2008; Liu et al., 2011), and heat activations are carried out at various temperatures (200 $^{\circ}$C – 1000 $^{\circ}$C) (Altundoğan et al., 2002; Liu et al., 2011). Processed bauxite and red mud may have different lattice structures and mineral phases compared to raw bauxite due to the activation processes (and the Bayer process). Examples for these mineral phase conversions are, original gibbsite ($Al(OH)_3$) to boehmite (γ-AlOOH), goethite (α-FeOOH) to hematite (α-Fe_2O_3), and titania minerals to perovskite (Altundoğan et al., 2002; Baral et al., 2007; Klauber & Power 2011). In addition to the minerals coming from original bauxite, red mud usually contains minerals like cancrinite, sodalite, and Ca-containing minerals as a result of the Bayer process. Cancrinite and hematite play major roles as effective metal-sorbing sites in red mud (Santona et al., 2006). Along with the structural transformations, the pore volume and the surface area of

modified bauxite are possibly higher due to removal of impurities improving the efficiency of the adsorption process. However, raw bauxite can be an effective sorbent of its own accord, and under certain conditions/environments it might perform better than its derivatives or similar sorbents. Since there is no activation or treatment with potentially hazardous chemicals, there is no risk of leaching of those substances to water or changing the chemical parameters of water in an adverse way. The minimum (almost non-existent) preparation and the implementation that do not require high-tech knowledge or plants, and high-cost labor also give cost benefits. Red mud particularly is considered a toxic industrial waste due to its high alkalinity (pH 10-13) and chemical characteristics (Hind et al., 1999), thus must be treated before use. Also, it may not be very practical to transport red mud sludge or processed bauxite to water treatment plants over a long distance without taking extreme measurements which might be costly and risky. Extra precautions will need to be taken in case of using them near public water sources due to potential leaching of chemicals. Especially in areas where there is a sufficient availability of raw bauxite, but the deposits are too low grade to be of any commercial value, bauxite might be an ideal candidate for a low-cost adsorbent that can be used locally.

The objectives of this research are to investigate the feasibility of raw bauxite to adsorb Pb^{2+}, Cu^{2+}, Ni^{2+}, and Co^{2+} in water and study the applicability of this method in lake water. While achieving this aim, I tested the effect of such parameters as the initial metal ion concentration, contact time between bauxite and polluted water, and the coexisting metal ions on the sorption efficiency of bauxite. In order to expand the study, I collected two compositionally different locally available bauxites and did a comparative study to find out if the type of bauxite has any effect on the overall performance, if so, which one is better, whether they have any preferences in sorption, and finally to understand the possible overall sorption mechanism.

CHAPTER 2 - SAMPLING AREA

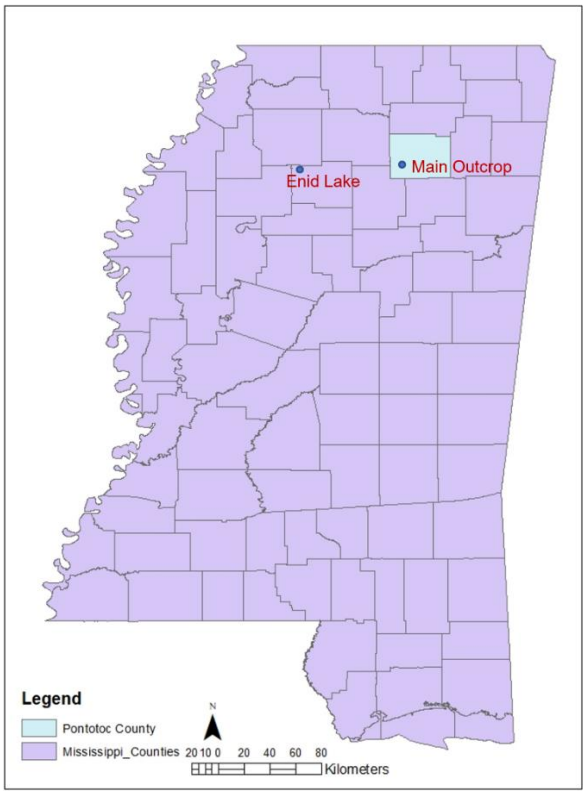

Figure 1. Sampling locations of bauxite and lake water

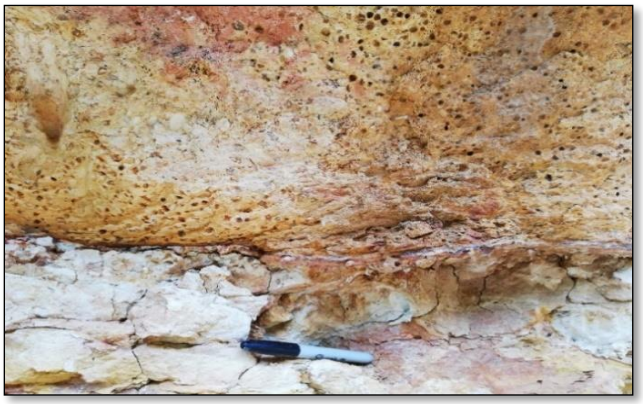

Figure 2. Bauxite in outcrop

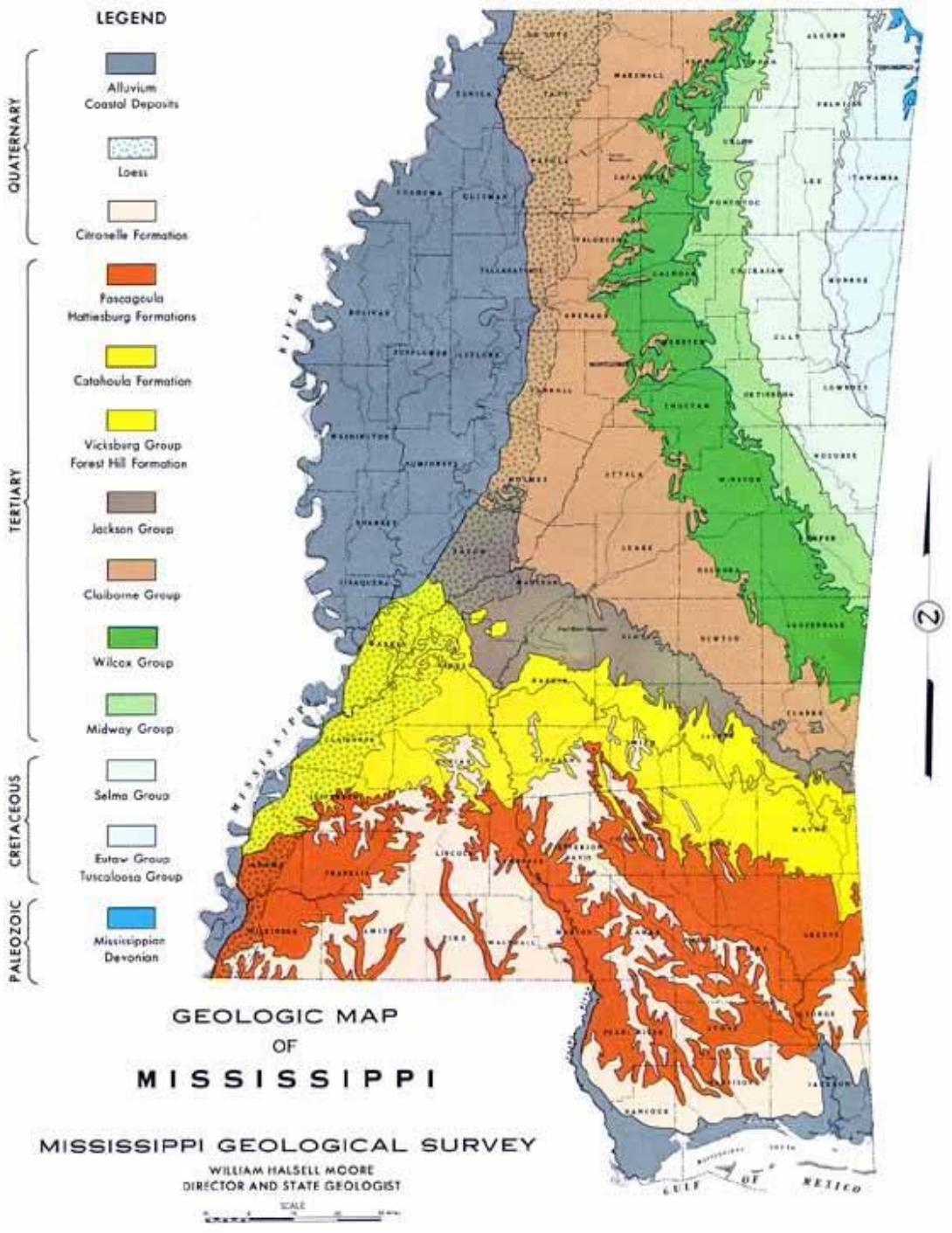

Figure 3. Geologic map of Mississippi (Bicker, 1969)

System	Series	Group	Stratigraphic Units			Description
Lower Tertiary	Lower Eocene	Wilcox	Mississippi (Northern)	Mississippi (Eastern)		
			Wilcox Group Undifferentiated	Hatchetigbee Formation		Interbedded sands, clays, carbonaceous clays, fissile shales and lignites
					Bashi Marl Member	Glauconitic, fossiliferous, sandy marl. Some lignite
	Paleocene			Tuscahoma Formation		Sands, thinly laminated locally, clays and fossil shales. Lignites are common. Locally at the base are large angular to rounded blocks of bedded silt.
				Nanafalia Formation		Clayey sand, silty clay, and clay - shales, Numerous lignite beds.
					Foam Spring Member	Laminated, silty, micaceous clay, and fine sand, thin lignites and reworked bauxitic material.
		Midway	Naheola Formation			Sand, carbonaceous clay - shales, laminated silts, and clays, kaolinitic and bauxitic clay found locally near the top.

Figure (continued)

			Porters Creek Formation	Porters Creek Formation	Matthews Landing Marl Member	Glauconitic, sandy clay, sparingly fossiliferous. Limonite concretions.
						Blocky clay, with slightly glauconitic, micaceous sand lenses. Siderite concretions. Tippah sand Lentil recognized in northern Mississippi as lenticular sands, clays, and sandstones.
			Clayton Formation			Glauconitic, laminated clays, marls, and sands. Locally fossiliferous.
				Chalybeate Limestone Member		Glauconitic, fossiliferous, sandy limestone, with interbedded fossiliferous marl.

Figure 4. Stratigraphy of the lower Tertiary northern-eastern Mississippi (Modified after Williamson, 1976 as cited in Thompson, 1989)

Raw bauxite was sampled from outcrops in Pontotoc County, Mississippi (Fig. 1, Fig. 2), which usually experiences a humid, temperate, moist climate. The average annual precipitation is 53 inches (Lane, 1973). Pontotoc County hosts most of the known bauxite deposits in Mississippi (Conant, 1949; Thompson, 1980). However, almost all the bauxite deposits in the state are of too low grade and compositionally variable to be economically mined (Conant, 1949; Thompson, 1980).

The bauxite deposits cover the stratigraphic range of the Upper Paleocene Midway Group – the Lower Wilcox Group (Thompson, 1980) (Fig. 3, Fig. 4). Paleocene strata in Mississippi are grouped into three formations: from oldest to youngest, the Clayton Formation, the Porters Creek clay, and the Naheola Formation of the Midway Group (Conant, 1949). In general, the Porters Creek clay is a massive black clay which can be lithologically categorized into three units. The upper-most unit is distinctively stratified compared to the lower units (Conant, 1949; Thompson, 1980). Crossbedded, fine-grained, micaceous sand and concretions of siderite (or limonite) are commonly seen in some layers and become more abundant upward (Conant, 1949). The upper member of the Porters Creek is considered as an equivalent to Naheola Formation (Thompson, 1980). The Porters Creek clay also consists of about 150-200 feet thick slightly lignitic clay (Buechakd, 1925). Bauxite deposits are mostly in the lower Ackerman Formation of the Wilcox Group (Buechakd, 1925). These deposits sometimes are underlain by (and part of) weathered top portion of the Porters Creek clay but, sometimes part of channel deposits that could be assigned to either the Porter Creek clay or the Wilcox Formation (Conant, 1949). The basal portions of the Ackerman Formation contain interbedded bauxite and clay which is not technically considered as kaolin due the abundance in fine-grained silica sand (Buechakd, 1925). Arguably, the contact between the Midway and Wilcox groups is unconformable (Buechakd, 1925; Conant, 1949). The deposits are commonly associated with lignite, lignitic clay and variegated sand of the base of the Wilcox Group (Morse, 1923; Burchard, 1924; Buechakd, 1925; Thompson, 1980).

Two main types of bauxite deposits can be identified in northern Mississippi: more common pisolitic, ferruginous/gibbsitic surface deposits and kaolinitc, sometimes pisolitic, gibbsite-poor subsurface deposits (Thompson, 1980). These ferruginous deposits with the Fe

content increasing upward usually regarded to have a lateritic origin and they are often exposed as resistant cap rocks (Thompson, 1980). There are several types of pisoliths seen in Mississippi deposits; gibbsite and goethite around quartz/mica nucleus, tiny clusters of kaolin and gibbsite oolites surrounded by goethite layer, and alternating goethite/kaolin and gibbsite layers nucleated around gibbsite (Thompson, 1980). The formation process of these pisolites could be influenced by groundwater circulation, colloids, organic matter, and electrolytes (Thompson, 1980).

Thompson (1980) mentions the possible mechanisms of bauxite formation in northern Mississippi that have been suggested by various researchers; in-situ formation due to sub-aerial leaching (desilication) of the Porters Creek clay that was caused by a regional Paleocene-Eocene unconformity (Mellen, 1939; Pandya, 1973), residual deposits produced by localized leaching processes (Priddy, 1943), channel and lagoonal deposits caused by shoaling of the Midway sea but an unknown process responsible for the formation of clay (Reed, 1952) etc. These concepts have been challenged time to time in the past.

In general, the Midway-Wilcox Groups in Mississippi represent a fluvial-deltaic sequence (Duplantis, 1975; Thompson, 1980). The marine conditions in the northern Mississippi Midway sediments (upper Porters Creek/Naheola equivalent) transitioned to swampy conditions, which then changed to fluvial-deltaic conditions (Conant, 1949; Thompson, 1980). The Al/Fe-rich deposits were of sedimentary origin and were possibly formed between the depositions of the shallow shelf and the incipient deltaic Porters Creek (and Naheola) sediments (Thompson, 1980). They were formed on low gradient deltaic and low energy tributary systems. Selective precipitation and/or differential flocculation must have removed Fe/Al-sediments from solution and settled (Thompson, 1980) forming the deposits. Early Wilcox strata were deposited following the late Paleocene incipient deltas resulting in the entire Midway system being covered

with fluvial-deltaic sediments. Progradation of these sediments was toward the west over the northern parts of the Mississippi Embayment (Thompson, 1980). Intense weathering and erosion over time exposed the parts of Al-rich Midway deposits (Conanat, 1949; Thompson, 1980). Some parts of these deposits became duricrust while the remainder stayed covered with Naheola/Lower Wilcox strata (Thompson, 1980). The exposed surfaces of the Midway system (Porters Creek) provided bases for the accumulation of lignitic clay and peat due to the abundant swampy settings (Conant, 1949). Sedimentary kaolin, which partially altered to bauxite also started accumulating locally (Conant, 1949). As a result, kaolin conglomerate channel deposits of the Wilcox found resting abruptly on the Porters Creek Clay could also be a parent of bauxite (Conant, 1949). Overall, bauxite, kaolin, lignitic clay, and all such related deposits in the area must have formed simultaneously in laterally adjacent interrelated environmental settings (Thompson, 1980).

CHAPTER 3 - METHODS

3.1. Field Methods

Several samples of bauxite were collected in the field, but the two 'types' of bauxite used in the experiments were sampled from an outcrop on Arrow Road, Pontotoc (Fig. 1, Fig. 2). The observed compositional/textural variation on the outcrop could be attributed to the changes in clay and Fe content. The base was more clayey, and the Fe content appeared to increase towards the top based on coloration. One of the samples (B1) used in the laboratory experiments was collected from the seemingly Fe-rich top portion of the outcrop and the other (B2) closer to the base.

In order to test the applicability of the suggested treatment method in a more natural environment, we decided to use lake water rather than distilled/deionized water as the matrix for all experiments. Lake water was sampled from Enid Lake, Mississippi (Fig. 1). The water samples were collected (pumped) closer to the shore, and distilled water cans washed several times with lake water were used as sampling containers. The lids were tightly closed, sealed with sealing films, and stored in the laboratory to be used later. Additionally, a sample filtered through a 0.45 µm filter (Proactive GoPro) and acidified with HNO_3 acid was collected in a laboratory plastic sampling bottle for cation analysis of lake water. All the water samples used in the experiments were collected during a single sampling trip. The pH of the water was ~6.55-7.01.

3.2. Analytical Methods

Bauxite samples were analyzed by X-ray Diffraction (XRD) using Cu-K radiation on a Rigaku MiniFlex X-ray diffractometer at the Department of Geology and Geological Engineering, University of Mississippi (UM). The scan speed and the step width were 2.00° 2Θ per minute and 0.01° respectively, and the patterns were recorded from 3~90° 2Θ. A Scanning Electron Microscope with Energy Dispersive X-ray Spectroscopy (SEM-EDS) at UM (JEOL JSM-7200FLV Field Emission Scanning Electron Microscope; Denton Desk V TSC Sputter Coater) was used to observe detailed morphology and quantify bulk chemical composition of both raw bauxites. The samples were examined at 15 kV accelerating voltage, around 10 mm working distance, and at different magnifications.

Ni^{2+}, Co^{2+}, Cu^{2+}, and Pb^{2+} ions, which have been popularly used in similar adsorption experiments were selected to test the ability of raw bauxite to remove them from solution. Two types of sorption experiments were carried out: single element experiments where only one desired metal was added to water, and multi-element (ME) experiments where all four metal ions were mixed. Stock solutions were prepared using 1000 mg/L of each standardized metal mixed in distilled water. All the chemicals used were of analytical grade. The parent solutions were further diluted to obtain the desired concentrations for practical use. Prior to using bauxite samples in the experiments, they were ground/powdered in a mortar, and sieved through a 63 µm (no. 230) mesh. No major modifications in the bulk structure are expected due to grinding/powdering process (Silva et al., 2009). The powdered samples were washed with distilled water to remove earthy materials (cleaned), filtered with P5 grade (Fisher brand) filter papers, and air-dried for several days.

Single-element solutions of metal ions were prepared at concentrations of 10, 100, and 500 ppb (µg/L) in lake water. 0.25 g of prepared bauxite powders were added to each metal solution to obtain a 1 g/L sorbent dosage. After vigorously shaking the flasks for ~1 minute, the solutions (with replicates) were left in contact with bauxite (both B1 and B2 series) over contact periods of 3, 6, 12, 24, and 48 hours. The experiments were performed at room temperature (25 $^{\circ}$C), and the pH of the systems was not controlled, thus reflecting ambient pH. Physicochemical conditions of the systems were not altered/maintained forcibly to mimic the environmentally relevant conditions and have the least external control over the reactions. After the predetermined contact period, the mixtures were filtered through 0.45 µm syringe filters. A portion of each filtered solution was diluted (10 ppb to 20 ppb, and 100 and 500 ppb to 5 ppb) in 10% nitric acid and analyzed for the respective element in an Inductively Coupled Plasma-Mass Spectrometer (ICP-MS) in the Department of Chemistry and Biochemistry at UM and Waypoint Analytical, Memphis. The same procedure was repeated for the ME-experiments. The only difference was, instead of having one target element in solution, the system contained all four metals. The variables of the experiments were the initial metal ion concentration in water, contact time, type of bauxite (B1 or B2), and the presence or absence of multiple metals in the system.

The amount sorbed was calculated from the concentration difference using the formula:

$$q_e = (C_o - C_e)\, V / W \qquad \text{Equation 1}$$

where q_e is the amount of metal ion adsorbed on the adsorbent, C_o, the initial metal ion concentration (µg/L), C_e, the equilibrium concentration of metal ion solution (µg/L), V, the volume of metal ion solution used (L), and W is the weight of adsorbent (air-dried bauxite) used (g).

The percentage adsorption was calculated using the formula:

$$\text{Percent adsorption} = ((C_o - C_e)/C_o)\ 100 \qquad \text{Equation 2}$$

where C_o, the initial metal ion concentration (µg/L), C_e, the equilibrium concentration of metal ion solution (µg/L).

The amount sorbed (metal uptake) and the percent adsorption values were plotted against contact time and initial metal ion concentration for each bauxite and each element in both single- and multi-metal systems. An attempt was made to analyze the data using the Langmuir and Freundlich isotherm models. The Langmuir model assumes uniform sorption energies on the surface of the substrate and no transmigration of sorbed ions in the plane of the sorbent surface (Adebowale et al., 2006). The Freundlich model states that at different concentrations, the ratio of the amount of sorbate sorbed onto a given mass of sorbent to the sorbate concentration in solution is not constant (Adebowale et al., 2006).

The non-linear Langmuir equation can be written as:

$$q_e = (Q^0 b C_e)/(1+bC_e) \qquad \text{Equation 3}$$

where q_e is the amount of sorbate sorbed per unit weight of sorbent (µg/g), C_e, the equilibrium concentration of the sorbate in solution (µg/L), Q^0, the monolayer adsorption capacity (µg/g), and b, the adsorption coefficient (L/µg).

The non-linear Freundlich equation can be written as:

$$q_e = K_F C_e^{1/n} \qquad \text{Equation 4}$$

where q_e is the amount of sorbate sorbed per unit weight of sorbent (µg/g), C_e, the equilibrium concentration of the sorbate in solution (µg/L), K_F, the Freundlich isotherm constant (µg/g), and

n, the Freundlich isotherm exponent. K_F is a measure of sorption capacity and n indicates the sorption intensity (Lavecchia et al., 2012).

CHAPTER 4 – RESULTS

4.1. Bauxite Characterization

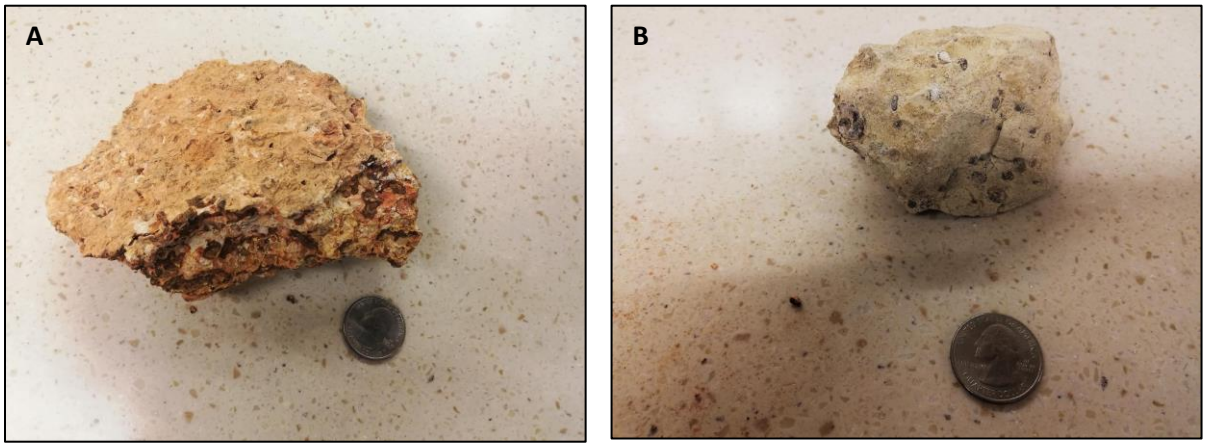

Figure 5. Two types of raw bauxite used for the experiments. **A)** B1. **B)** B2. (a US quarter for scale).

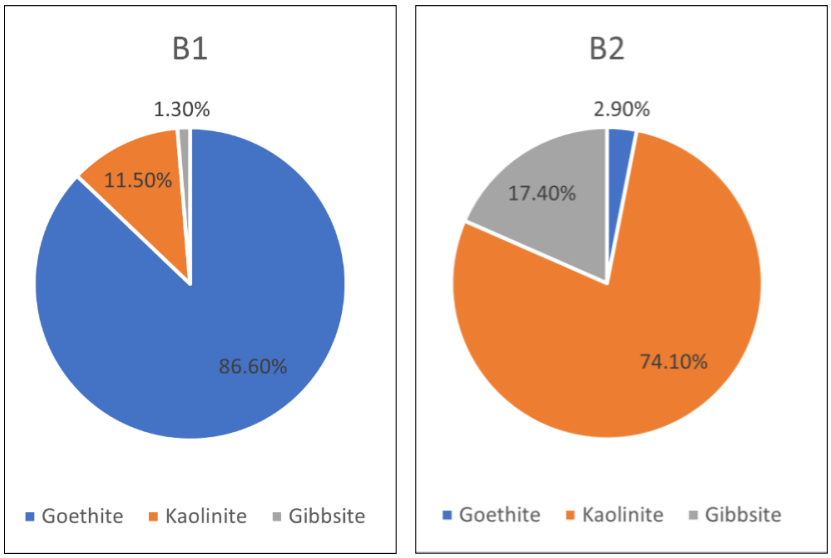

Figure 6. Major mineral compositions of B1 and B2 (XRD analysis)

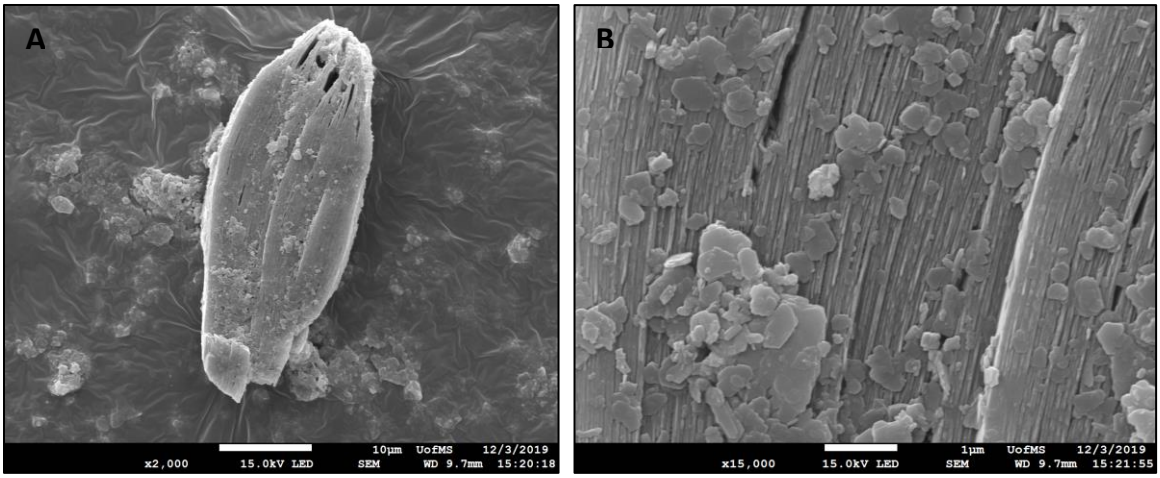

Figure 7. Bauxite under SEM (Secondary Electron). **A)** Magnification x2000. **B)** Magnification x15000

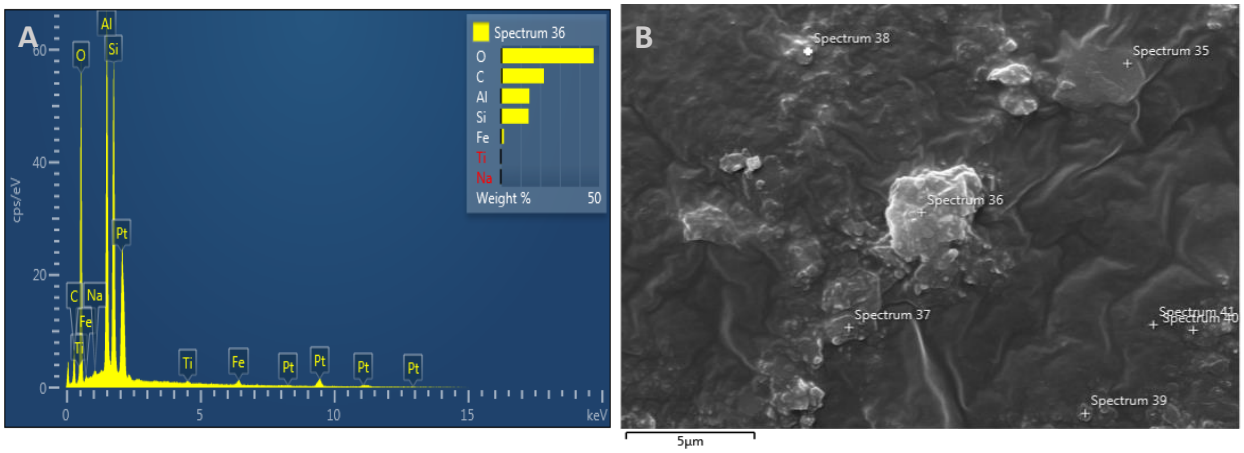

Figure 8. An example SEM-EDS spectrum of Bauxite. (A) is the generated spectrum for the corresponding point on (B)

The two bauxite hand specimens show compositional differences (Fig. 5). B1, collected from a seemingly Fe-rich part of the outcrop, is more reddish brown in color and has a mottled appearance. B2 which was sampled closer to clayey base of the outcrop is white-brown color with a few pisoliths. According to the XRD results (Fig. 6), B1 is mainly composed of goethite (~86.6%), kaolinite (~11.5%), gibbsite (~1.3%), anatase (~0.58%), and hematite (~0.0038%),

while B2 mostly consists of kaolinite (74.1%), gibbsite (17.4%), and goethite (2.9%). SEM-EDS detected higher concentrations of Al, Fe, S, Si, and O with minor amounts of Ti, Na, and K in bauxite (Fig. 8). The analysis of Pb^{2+} treated bauxite confirmed the presence of trapped-Pb in bauxite, however, the SEM analysis did not confirm the presence of Pb in untreated raw bauxite.

4.2. The Effect of Initial Metal Ion Concentration

Pb^{2+} adsorption by both B1 and B2 show similar trends for 3, 6, and 48-hour contact times (Fig. 9A; Tables 5-6, Appendix). All three sets of solutions have the highest percent adsorptions (81-94% for B1 and ~96% for B2) at the initial concentration of 100 ppb and the lowest at the initial concentration of 500 ppb (~12-31% for B1 and ~45-56% for B2). For both bauxites, the percent adsorptions at 12 and 24-hour periods are less than the rest of the experiments, and their percent adsorption values do not tend to fluctuate significantly. Cu^{2+} adsorption by both bauxite types shows similarities in the adsorption patterns with respect to the initial concentration of metals, especially at the 3- and 6-hour contact times (Fig. 9B). Adsorption by B1 at 3 hours is slightly higher than at 6 hours. Both bauxites show a significant drop in percent adsorption (B1 from ~90% to 20% and B2 from ~ 75-85% to 20%) at 500 ppb, for both 3- and 6-hour periods (Fig. 9B; Tables 5-6, Appendix). The adsorption pattern of Cu^{2+} for 12-hour samples closely follows that of the 6-hour samples. Also, adsorption by B2 after 24 hours is almost 100% for both 10 ppb and 100 ppb solutions. B1 does not show a high percent adsorption at 10 ppb, but it shows removal of Cu^{2+} almost completely at 100 ppb. Cu^{2+} in contact with bauxites was reported below detection limits at 48 hours, and at 24 hours for 500 ppb solutions. The trend was similar for Cu^{2+} solutions in B2 at 12 hours. For 3, 6, and 48-hour contact times, Co^{2+} shows the highest percent adsorption (~30-80% for B1 and 31-67% for B2)

at 10 ppb and the lowest at 500 ppb (~3-17% for B1 and 6-18% for B2) (Fig. 9D; Tables 5-6, Appendix). Unlike the 6- and 48-hour series, the percent adsorption of the 3-hour series decreases gradually between 10 ppb and 500 ppb. The 12- and 24-hour series of both bauxites have the highest percent adsorptions (~49-78% for B1 and ~50-80% for B2) at 100 ppb and the lowest at 500 ppb (~15%).

Overall Pb^{2+} uptake by bauxite increases with initial metal concentration in water (Fig. 10A; Tables 9-10, Appendix). They do not show exponential or linear relationships. For B1, the increment between 100 ppb and 500 ppb is lower than that between 10 ppb and 100 ppb (the slope decreases). At the 3-hour and the 6-hour contact times the uptake decreases from 0.082 mg/g and 0.093 mg/g at 100 ppb to 0.063 mg/g and 0.069 mg/g at 500ppb. However, the uptake always increased between 10 ppb and 100 ppb. Pb^{2+} uptake by B2 increases with sorbate concentration at all the contact times. Even though there is a slight decrease in increment in uptake from 100 ppb to 500 ppb, the uptake values of B2 at 500 ppb (0.228 mg/g-0.285 mg/g) are higher than those of B1 (0.063 mg/g-0.158 mg/g). The differences in uptake values at 10 ppb and 100 ppb are not very pronounced even though B2 shows slightly higher values. Cu^{2+} uptake increases with the initial metal concentration in solution (Fig. 10B). Considering the increase in initial concentration of solution, the increment in uptake from 100 ppb to 500 ppb is low. Excluding the inferred values due to no detection, uptake is 0.004 mg/g - 0.009 mg/g at 10 ppb, 0.086 mg/g - 0.098 mg/g at 100 ppb, and 0.100 mg/g - 0.125 mg/g. The uptake values for B2 are roughly comparable to those of B1. However, Cu^{2+} was often reported below detection limits at the 12-48 contact periods. Considering the reported values for the 3-hour and the 6-hour contact times, it shows a decrease in value between 100 ppb and 500 ppb (Fig. 10B; Tables 9-10, Appendix). Especially at longer contact times, calculated values show negative Ni^{2+} uptakes

(Fig. 10C; Tables 9-10, Appendix). However, at shorter contact times, the uptake by B1 increases with sorbate concentration. The increment is non-linear, and the slope decreases between 100 ppb and 500 ppb (0.003 mg/g-0.007 mg/g at 10ppb to 0.029 mg/g-0.068 mg/g at 100 ppb to 0.079 mg/g-0.095 mg/g at 500 ppb). B2 also shows a similar trend (0.004 mg/g-0.006 mg/g at 10 ppb to 0.021 mg/g-0.066 mg/g at 100 ppb to 0.093 mg/g-0.14 mg/g at 500 ppb). Co^{2+} uptake by B1 increases between 10 ppb and 100 ppb but, a noticeable increment in uptake between 100 ppb and 500 ppb is observed only at 3-hour (0.029 mg/g to 0.088 mg/g) and 48-hour (0.038 mg/g to 0.63 mg/g) experiments (Fig. 10D; Tables 9-10, Appendix). The uptake of Co^{2+} remains almost unchanged at 12-hour and 24-hour experiments. At the 6-hour contact time, the uptake shows a decrease (0.03 mg/g at 100 ppb to 0.019 at 500 ppb). The uptake of Co^{2+} by B2 increases between 10 ppb and 100 ppb at all contact times. A noticeable increment in uptake between 100 ppb and 500 ppb initial concentration levels is observed only at the 3-hour (0.031 mg/g to 0.089 mg/g) and the 48-hour (0.051mg/g to 0.092 mg/g) experiments. At the 6-hour and the 12-hour contact times, uptake of Co^{2+} increases slightly, but the samples at the 24-hour contact time show a slight decrease in uptake (0.080 mg/g at 100 ppb to 0.074 mg/g at 500 ppb).

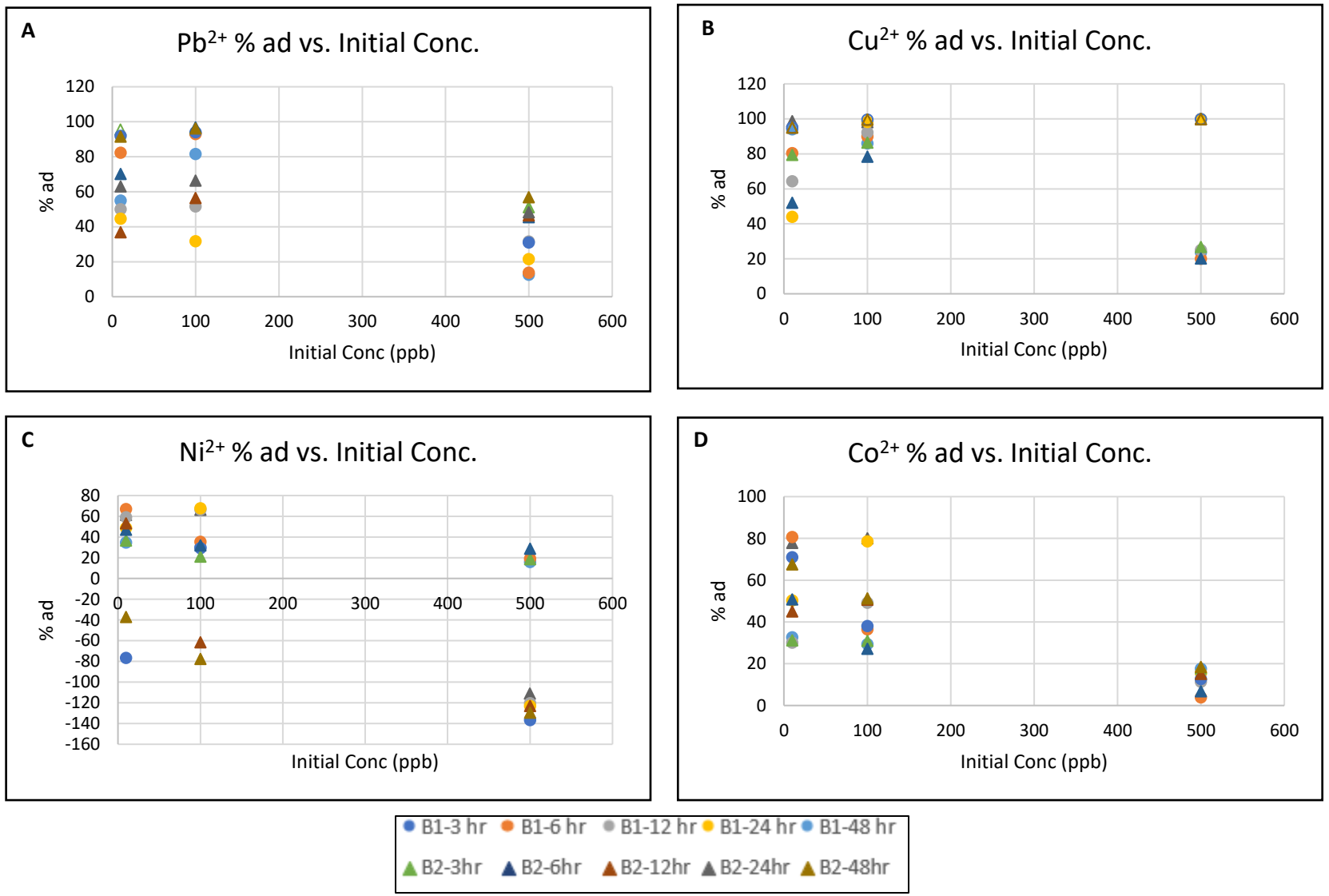

Figure 9. Adsorption Percentage (% ad) vs. Initial Concentration (initial conc) of each metal in the single-element solutions. A) Pb^{2+}. B) Cu^{2+}. C) Ni^{2+}. D) Co^{2+}.

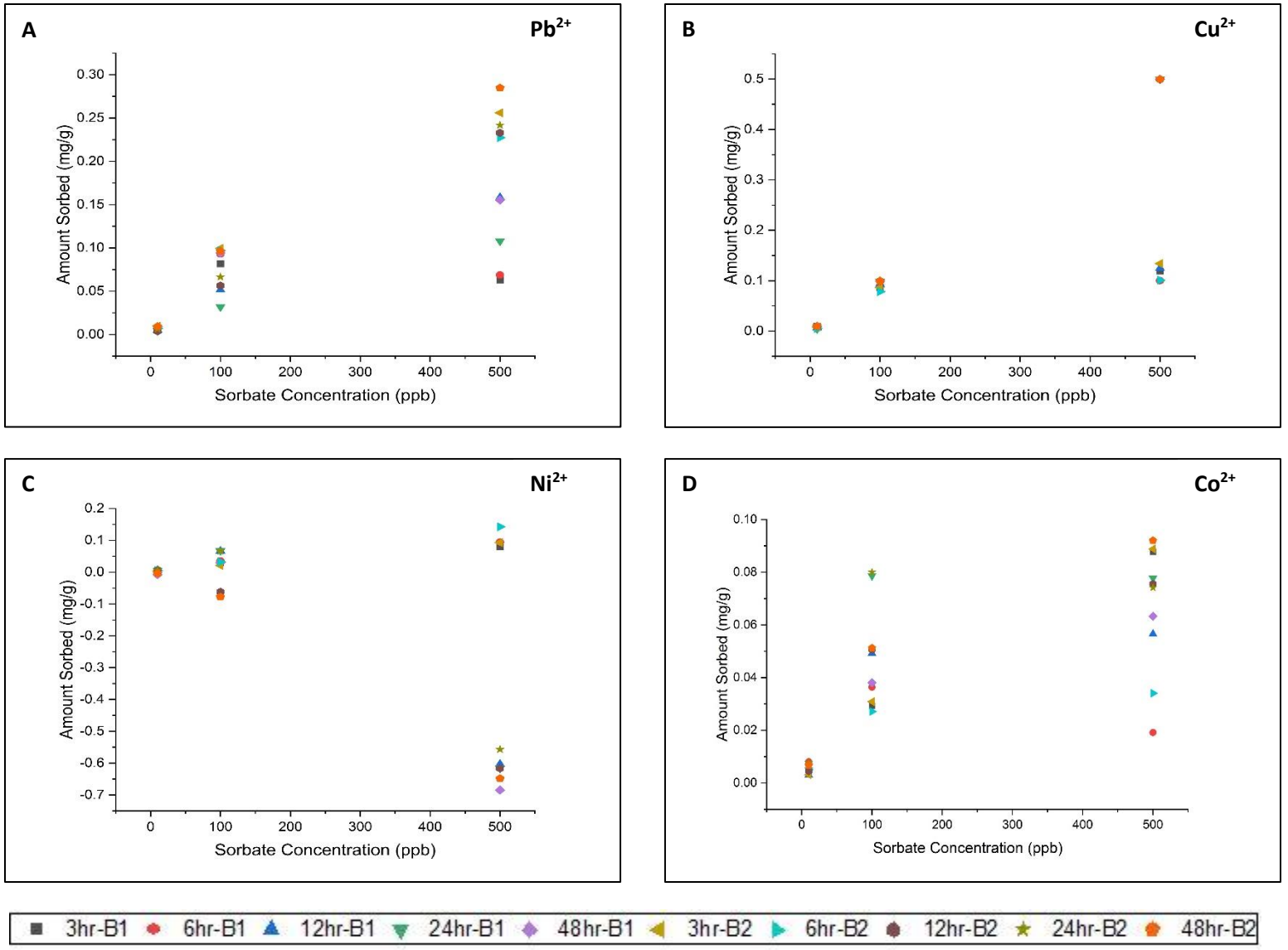

Figure 10. Uptake vs. sorbate concentration for each metal in the single-element solutions. A) Pb^{2+}. B) Cu^{2+}. C) Ni^{2+}. D) Co^{2+}.

4.3. Adsorption Isotherms

Sorption data show better correlation with the Langmuir isotherm model (Fig. 16-17, Appendix; Tables 13-16, Appendix). Strong statistical parameters were generated during curve fitting (e.g., R^2 (COD)) due to lack of data points. Also, it was impossible to run statistical tests as they would not prefer any model due to there being very few data points available. However, considering the overall correlation pattern, and especially the shapes of the curves, it can be assumed that data follow the Langmuir adsorption model. Generally, Cu^{2+} shows the highest calculated Q_{max} values followed by Pb^{2+} and Co^{2+} (Ni^{2+} is excluded due to negative data points). The Freundlich *n* values are around 1-2, but Co^{2+} especially shows relatively higher values.

4.4. The Effect of Contact Time

Both bauxites are more efficient in removing lower concentration-Pb^{2+} (10 ppb and 100 ppb) after ~6 hours and ~48 hours (Fig. 11A). At 500 ppb, B1 adsorbs more around the 3-hour and the 48-hour times, and B2 at the 12-hour and the 48-hour times. The variation in percent adsorption with time is much less for 500-ppb samples compared to the ones at lower concentrations (~12-30% for B1 and ~45-55% for B2). B2, in particular, exhibits very mild fluctuations. Overall, Cu^{2+} adsorption tends to peak around 12-24 hours and remain constant (Fig. 11B). Often, there seems to be an initial decline (from 3 hours to 6 hours) followed by an increment in the percent adsorption. Except B1 with 10 ppb Co^{2+}, both bauxites show the highest adsorption for Co^{2+}efficiencies around 24 hours. (Fig. 11D). Generally, all these bauxite-metal systems tend to attain their peak percent adsorption around 12-24 hours.

Metal uptake data for both bauxites do not follow considerable trends at 10 ppb and 100 ppb concentrations (Fig. 12). At both 10 ppb and 100 ppb initial metal concentrations, Pb^{2+}

uptake decreases after 6 hours for B1 and after 3 hours for B2, but both showed higher uptakes again at the 48-hour contact time. The lowest uptake values were reported at the 24 hours for B1 (0.004 mg/g at 10 ppb and 0.032 mg/g at 100 ppb) and the 12 hours for B2 (0.004 mg/g at 10 ppb and 0.056 mg/g at 100 ppb). Considering the reported values, Cu^{2+} uptake showed a slight decline at 6 hours but tends to increase afterwards. Overall, the uptake decreases with time (at least at the beginning) at 10 ppb but increases at 100 ppb concentrations. Excluding the reported negative values, overall Ni^{2+} uptake values were higher around the 24-hour contact time. Except in B1- 10 ppb solutions, at 10 and 100 ppb initial metal concentrations, Co^{2+} shows the highest uptakes around 24 hours and a slight decline after. Even though Cu^{2+} data were often reported below detection limits, and Ni^{2+} showed negative values, Pb^{2+} (linear intercept: 0.079 mg/g for B1 and 0.231mg/g for B2) and Co^{2+} (0.057 mg/g for B1 and 0.062 mg/g for B2) clearly show less fluctuations in uptake with contact time. At 500 ppb, particularly Pb^{2+} and Co^{2+} show less fluctuations in uptake/tendency to attain a constant value with time (Pb^{2+} 0.11-0.15 mg/g in B1, 0.23-0.28 mg/g in B2 and Co^{2+} 0.057-0.078 mg/g in B1, 0.075-0.092 mg/g).

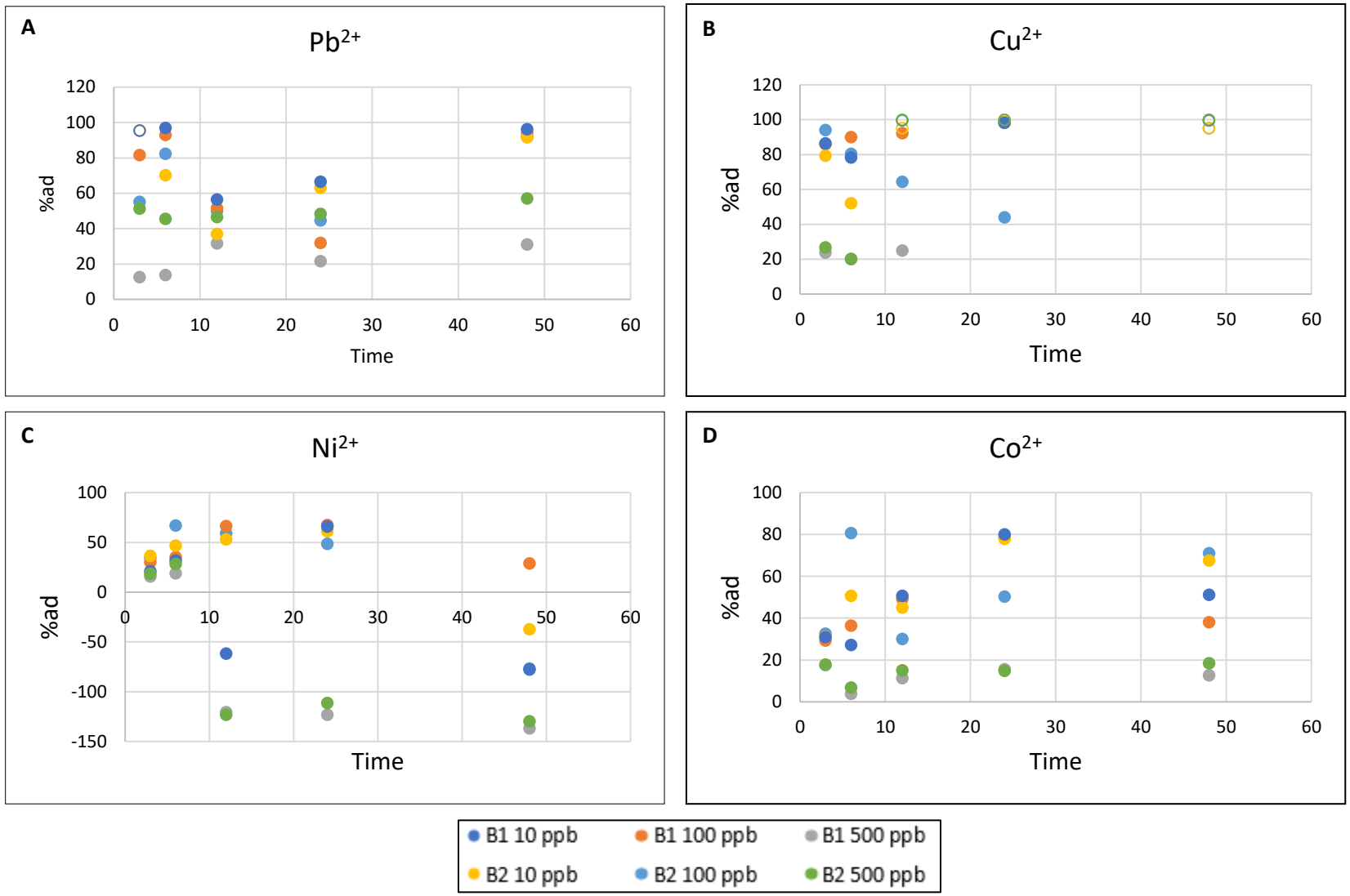

Figure 11. Percent adsorption vs. contact time for each metal in the single-element solutions. A) Pb^{2+}. B) Cu^{2+}. C) Ni^{2+}. D) Co^{2+}.

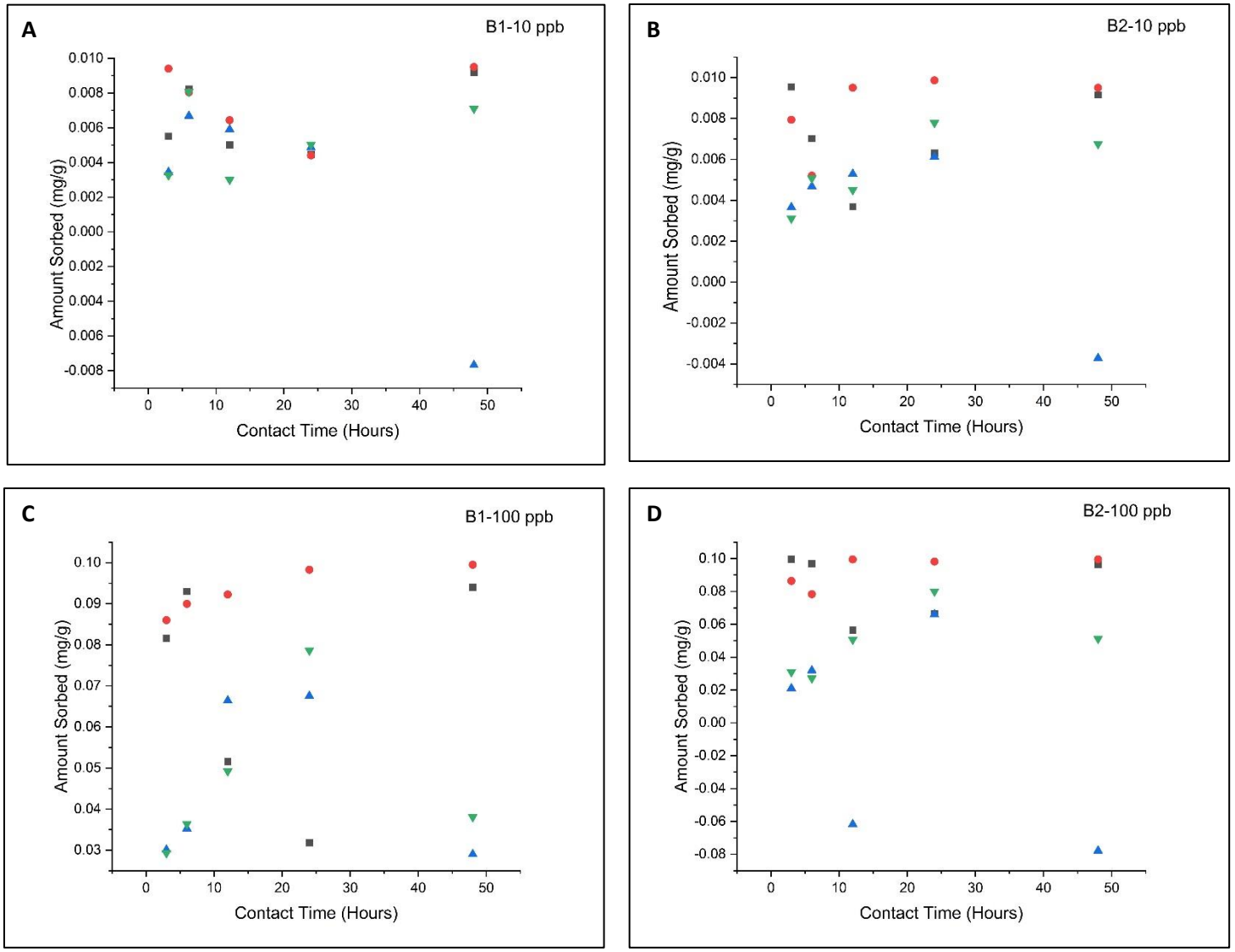

Figure (continued)

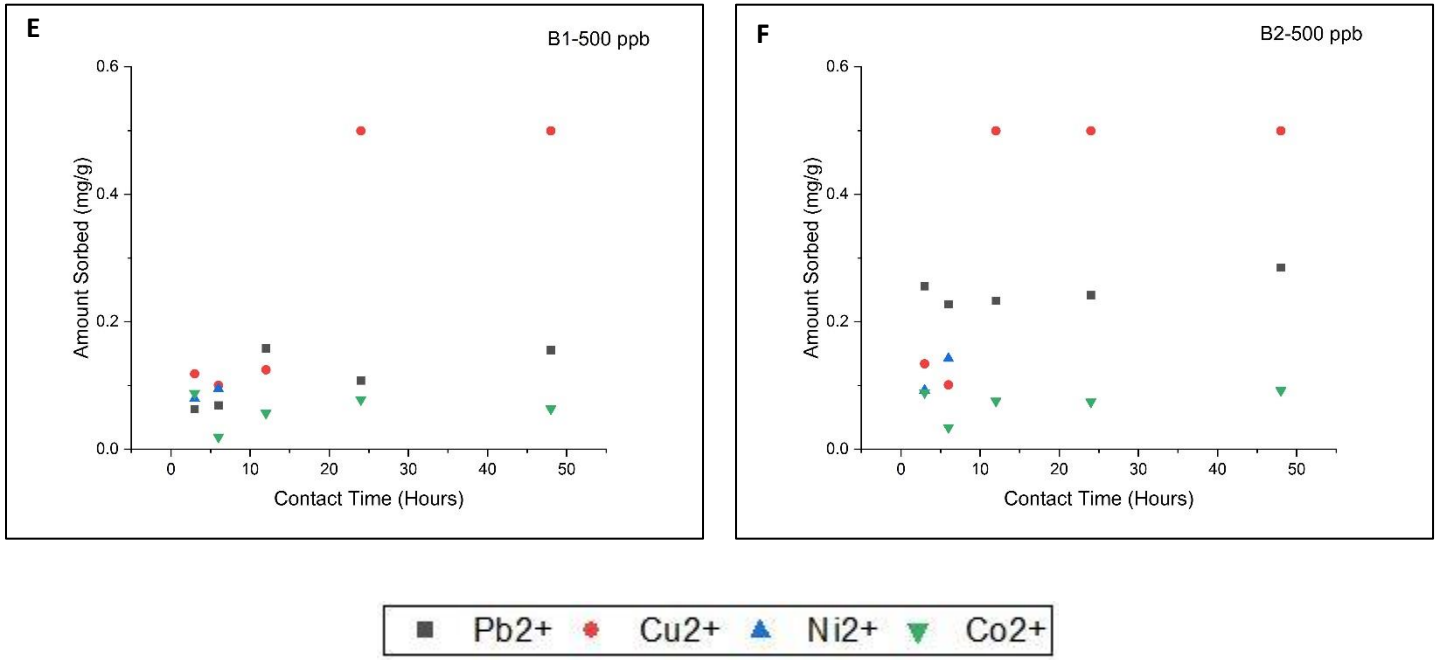

Figure 12. Uptake of metals in the single-element solutions by B1 and B2 at each sorbate concentration vs. contact time. A) B1-10 ppb. B) B2-10 ppb. C) B1-100 ppb. D) B2-100 ppb. E) B1-500 ppb. F) B2-500 ppb.

4.5. The Effect of the Presence of 'Other' Metal Ions

Adsorption of Pb^{2+} and Cu^{2+} in ME solutions do not show the same trends as those for their single-element solutions (Fig. 13A; Tables 7-8, Appendix). The final concentrations for the samples with initial concentration of 10 ppb were often reported below detection limits. Overall, for any given contact time, Pb^{2+} shows the lowest adsorption (near 0% for B1 and ~2-10% for B2) at 500 ppb initial concentration. Cu^{2+} generally has the same trend but, after certain contact periods (e.g., B2-6 hours), 500 ppb concentrations showed a slightly higher adsorption relative to 10 ppb or 100 ppb (Fig. 13B). None of the samples that were tested for Ni^{2+} reported negative percent adsorption values (Fig. 13C; Tables 7-8, Appendix). Ni^{2+} and Co^{2+} show almost similar trends in adsorption (Fig. 13C-D). For lower initial concentrations, percent adsorptions of the 3-, 6-, and 48-hour series are fairly low relative to the 12- and 24-hour series (except for ME B1 Co^{2+} at 10 ppb). Significant decreases in adsorption at 500 ppb concentrations cannot be noticed for these solutions. Both Ni^{2+} and Co^{2+} show the highest percent adsorption at 100 ppb for both the 12- and 24-hour series and the lowest at 500 ppb. In the ME experiments, Ni^{2+} and Co^{2+} showed higher consistency in terms of both contact time and initial concentration.

Overall, the Pb^{2+} uptake increases then decreases with initial metal ion concentration (Fig. 14A). Cu^{2+} uptake increases with initial metal concentration at some contact times (e.g., 3-hour) or shows a decrease at 500 ppb (e.g., 24 hours). In case where uptake continuously increases with concentration, the increase in uptake at 500 ppb is low (B1-12 hours) especially in solutions in contact with B1 (Fig. 14B). Some of B2 samples show higher uptake values at 500 ppb (3 hours and 6 hours). Ni^{2+} uptake increases with initial metal concentration (Fig. 14C). The increment is not very significant in some samples (e.g., 24 hours). Except in B1-12-hour, B2-12-

hour, and B2-24-hour samples, Co^{2+} uptake increases with initial metal concentration in solution (Fig. 14D).

Generally, Pb^{2+} and Cu^{2+} show decrease in percent adsorption with time, then increase after ~6 -12 hours, and remain almost constant or decrease (Tables 7-8, Appendix). Adsorptions of Ni^{2+} and Co^{2+} especially at lower concentrations increase with time, after ~6 hours until 24 hours and decrease, except B1-10 ppb which peaked at 6 hours and 24 hours. Variations in percent adsorption of metals at 500 ppb are low for both bauxites. In general, Pb^{2+} uptake with contact time fluctuates slightly around 0.026 mg/g for B1 and 0.052mg/g for B2 (Fig. 15; Tables 11-12, Appendix). A decrease in Cu^{2+} uptake around 6-12 hours and an increase afterward were observed at 10 ppb and 100 ppb metal-bauxite systems (both B1 and B2). For 100 ppb metal solutions, the peak uptakes are at 24-hour contact time (0.097 mg/g for B1 and 0.067 mg/g for B2). At 10 ppb and 100 ppb initial metal concentrations, Ni^{2+} uptake at 3, 6, and 48-hour contact times are comparable in each system (0.002 mg/g in B1 at 10 ppb, 0.002 mg/g-0.003 mg/g in B2 at 10 ppb, 0.011 mg/g-0.017 mg/g in B1 at 100 ppb, and 0.014 mg/g-0.017 mg/g in B2 at 100 ppb). The peak uptakes are at 24 hours (0.006 mg/g in B1-10 ppb, 0.006 mg/g in B2-10 ppb, 0.07 mg/g in B1-100 ppb, and 0.06 mg/g in B2-100 ppb). Overall, Co^{2+} uptake by both bauxites in 10 ppb and 100 ppb metal solutions show similar trends with contact time. Except in B1-10 ppb, the uptake decreases between 3 hours and 6 hours, then increases until 24 hours, and decreases afterwards. At 500 ppb, Ni^{2+} shows two increments in uptake by B2 at the 12 hours and the 48 hours but for B1 the peak uptake is at the 12 hours (0.094 mg/g), and the uptake is constant at the 24 hours (0.075 mg/g) and the 48 hours (0.076 mg/g). Co^{2+} uptake onto B2 seems almost constant (around 0.047 mg/g), but B1 shows a decrease in uptake at 6 hours and 48 hours. In

general, Cu^{2+} shows a decrease in uptake with contact time. Pb^{2+} shows uptake values closer to zero (Fig. 15).

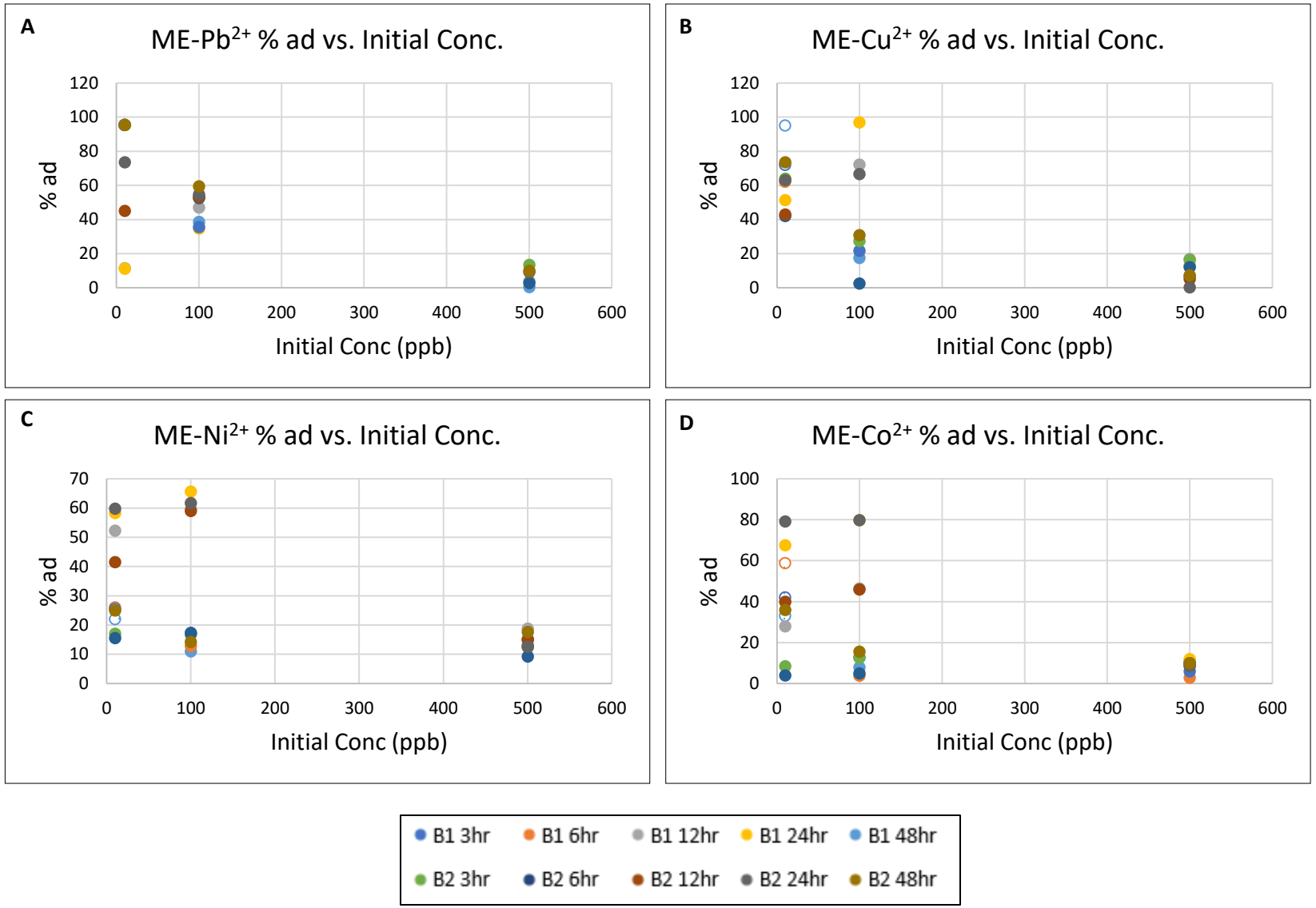

Figure 13. Percent adsorption vs. contact time for each metal in the multi-element solutions. A) Pb^{2+}. B) Cu^{2+}. C) Ni^{2+}. D) Co^{2+}.

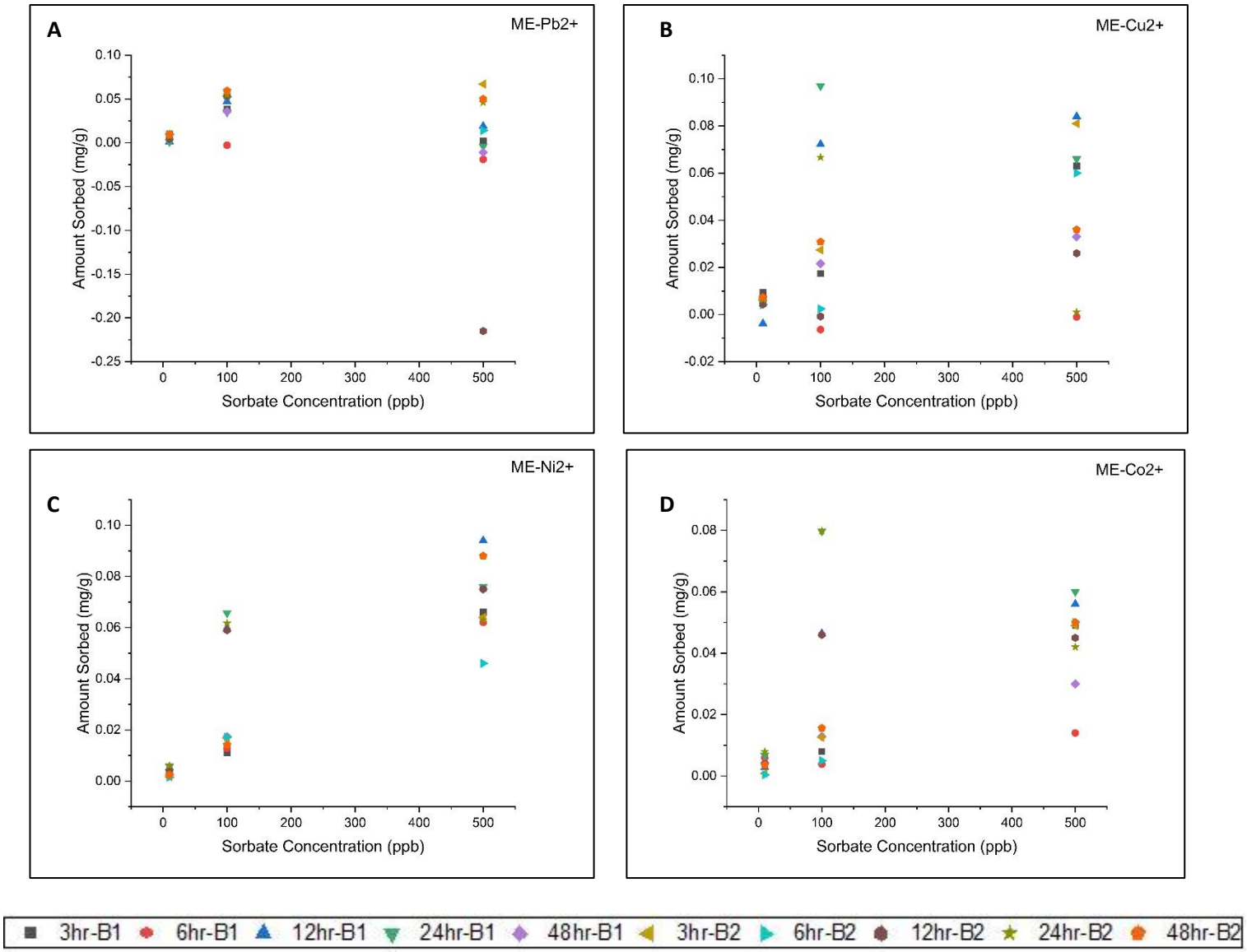

Figure 14. Uptake of metals vs. sorbate concentration for each metal in the multi-element solutions. A) Pb^{2+}. B) Cu^{2+}. C) Ni^{2+}. D) Co^{2+}.

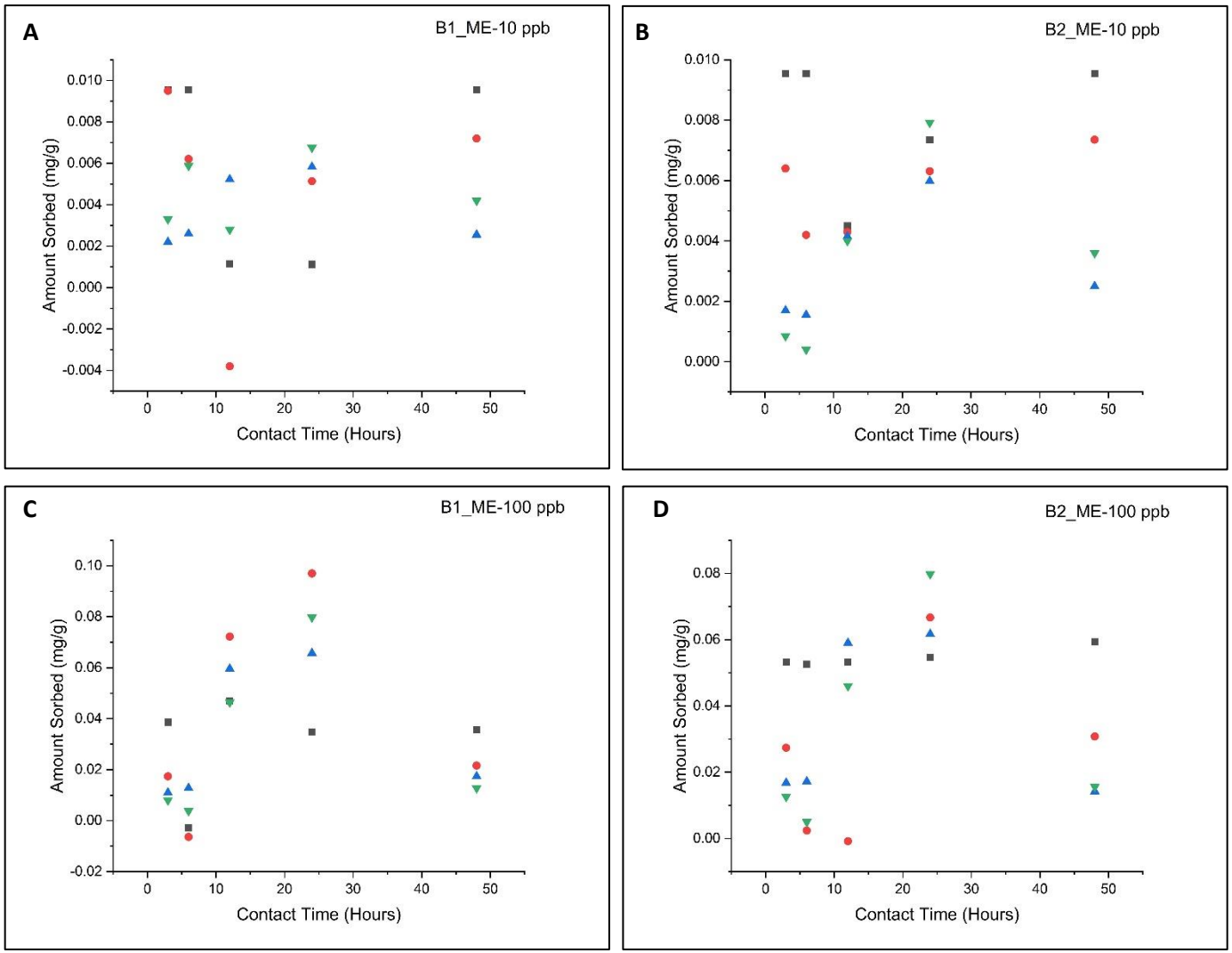

Figure (continued)

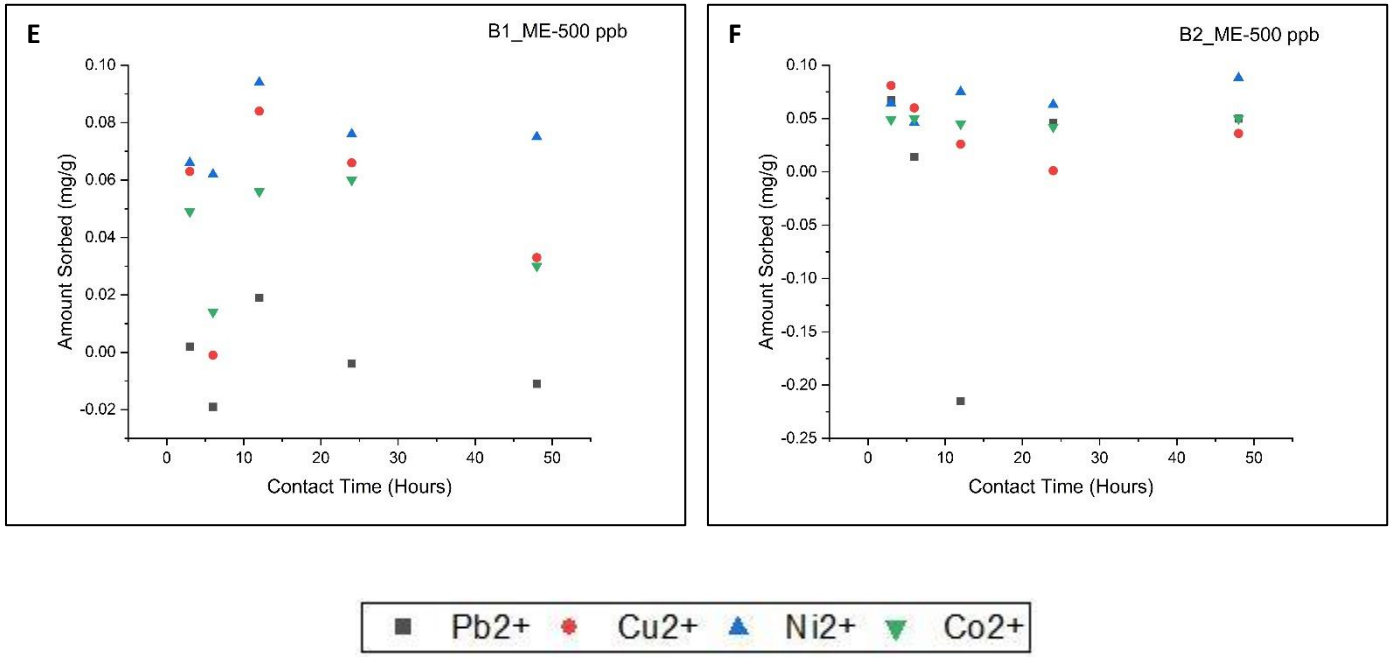

Figure 15. Uptake by B1 and B2 at each sorbate concentration vs. contact time metals in the multi-element solutions. A) B1-10 ppb. B) B2-10 ppb. C) B1-100 ppb. D) B2-100 ppb. E) B1-500 ppb. F) B2-500 ppb.

CHAPTER 5 - DISCUSSION

5.1. Metal Sorption by Bauxite, Possible Sorption Sites, and Mechanisms

Except in certain Ni^{2+} containing systems, both bauxites showed a noticeable removal effect on metals. Bauxite has 'layered (channel-like)', porous structure and rough surfaces, increasing the surface area (Fig. 7). Features such as irregularly broken edges and kinks can enhance site heterogeneities on sorbent surfaces resulting in different specific binding energies at different surface sorption sites (Manning & Goldberg, 1996). Also, rough surfaces can give solid contact for metals and the sorbents. Clay surfaces, hydroxide, and oxide surfaces (e.g., Al_2O_3, Fe_2O, and $TiO_{2)}$ in bauxite are the possible adsorption sites for heavy metals. Physical characteristics such as high charge/mass and surface/volume ratios enhance the binding capacity of bauxite and favor the diffusion of metals into bauxite (Grim, 1962; Altundoğan et al., 2002; Genç et al., 2003; Liu et al., 2011; Lee et al., 2017; Uddin, 2017). Large concentrations of Fe and Al minerals accommodate surface sites for sorption mechanisms. Silicate minerals usually have large specific areas of bonding such as [AlO—], [Si—O—] that can be easily charged and bonded with metal ions, covering the surface (Ouyang et al., 2019). The surface charge of mineral species occurs through ionization of surface groups. The potential difference created allows the ions to approach the surface.

Bauxite samples are composed of a complex mixture of minerals such as gibbsite, goethite, kaolinite, anatase and hematite (hence they do not have fixed compositions). A complete understanding of heavy metal removal by bauxite is currently lacking. However, the

sorption behavior of these individual species has been studied by many researchers. The goal of my study was to understand the sorption behavior of bauxite by focusing on these individual species, finding possible relationships, and applying where they coexist. Also, the main compositional differences in the two samples I used in this study were in their Fe content and clay content. B1 was Fe rich (goethite) while B2 was clay rich (kaolinite). The initial metal ion concentration seems to have a slightly higher effect on adsorption by B1 compared to that by B2. B2 seems to be a better sorbent due to its slightly higher removal efficiencies. The observed slight differences in their performance could be attributed to this major compositional difference.

Goethite octahedra (each with six oxygens coordinated to the central Fe (III)) share oxygen atoms to form two rows of two octahedra. Interconnected at the corners, these rows act as being surrounded by open channels. These channels occupied by protons act as grooves on the outside to trap ions (Russell et al., 1974). The presence of singly or doubly coordinated oxygens at the surface can readily bind heavy metals via inner-sphere complexes for charge compensation. These surface oxygens behave as amphoteric acids. Kaolinite is a 1:1 type layer silicate, which consists of one tetrahedral silica sheet alternating with an octahedral alumina sheet sharing a common plane of oxygen atoms within a layer. Kaolinite has strong bonding and no interlayer swelling. The structure is well-kept by hydrogen bonding and Van der Waals forces (Bear, 1965; Uddin, 2017). This structure allows silica-oxygen and alumina-hydroxyl sheets to be exposed to different substances in the surrounding (Grim, 1968). Kaolinite has the potential to remove heavy metals in water mainly through adsorption and ion-exchange mechanisms (Jiang et al., 2010; Uddin, 2017). As the structure is tightly packed and the bonding is so strong, the sorption mechanisms most probably take place along the edges and on the surface.

Clays are usually considered as potential adsorbents due to the high specific area, layered structure, chemical and mechanical stability, Brönstead and Lewis acidity, and high cation exchange capacity (CEC) (Tanabe, 1981). Negatively charged sites on clay particles could attract positively charged ions (Atasoy & Bilgic, 2018). However, their role in adsorbing heavy metals is not significant compared to the oxides. Among clay minerals, kaolinite in particular has a relatively smaller surface area and low CEC (Jiang et al., 2010). However, in this work, B2 with significantly higher kaolinite content showed higher uptake and removal efficiencies in general. Considering the genesis, kaolinite in the samples used in this study may not be considered as typical kaolinite, and it should contain large amounts of fine-grained Fe-oxyhydroxides and other impurities. If kaolinite is contaminated, the CEC can be inflated, and the metal uptake may not represent the true CEC. Studies have shown that illite (Fe-containing clay) or Fe oxide contamination in kaolinite can increase the CEC and the specific surface area (Tschapek et al., 1974; Yong et al., 1992; Balan et al., 1999). Such contaminants can cause structural modifications, possibly allowing molecules to move more freely. This combined effect must have enhanced the capability of metal retention by B2 greatly. Also, it is expected that the input from organic matter (e.g., lignite seams in the area) in the bauxite composition is not negligible. Organic ligands can act as complexants and redox agents influencing metal mobility (Bermond & Bourgeois, 1992). CEC can be highly influenced especially by the organic matter-clay particle interactions (Parfitt et al., 1995; Ma & Eggleton, 1999; Soares & Alleoni, 2008). However, loss on ignition data would be helpful in conforming how significant the contribution by organic matter in sorption. Natural water can also contain naturally occurring organic matter which may either augment mobility of metal ions via aqua-metal-organic complexation or enhance the adsorption process by forming ternary metal-organic-surface complexes (Boily & Fein, 1996).

Therefore, the overall sorption capacity of bauxite can be attributed to clay minerals, oxyhydroxide, and the organic content.

The sorption process on bauxite could be a collective of many mechanisms and these processes could be sequential. It could generally be considered that chemisorption is the main retention mechanism of metals on Fe-oxides, and adsorption and ion exchange onto clays (Friesl et al., 2006; Jiang et al., 2010; Uddin, 2017). However, studies have found that more than one stoichiometric surface reaction is needed to describe metal adsorption mechanism, suggesting the involvement of more than one type of surface sites in sorbing more than one type of species (Davis & Leckie, 1978; Spark et al., 1995; Rodda et al., 1996). So, the overall mechanisms of sorption may not be a simple process. Various theories such as the Gouy-Chapman-Stern Graham model on electrostatic adsorptions, the adsorption-hydrolysis model, the ion-solvent interaction model, the ion exchange model, and the surface complex formation model have been introduced to understand metal adsorption particularly onto hydrous oxide surfaces (Stumm et al., 1976). Most of the theories are usually developed based on experimental data using individual species, thus applications on natural material may lead to complications. Compared to well-defined mineral species, natural materials are usually composites of several mineral phases and matter.

Especially due to the heterogeneity of the rock, it is possible that several sorption processes such as precipitation, diffusion, surface complexation, and surface sorption contribute to metal removal from water (Singh et al., 2001). Overall, chemisorption seems to be the dominant mechanism accounting for metal immobilization. Especially at lower sorbate concentrations, chemisorption along with physical adsorption should play major roles in sorption. When the sorbent has capacity for additional sorption, metals may load usually via

loose bonds onto easily reducible and exchangeable phases (Saeedi et al., 2013). At higher metal concentrations in water, reactions such as precipitation can occur. Precipitation can form less readily desorbed solid phases. As a combined effect, uptake would increase with increase in sorbate concentrations. Even though it was not consistently observed in all the samples, some of the samples showed tendencies to decline in uptake at higher metal concentrations in solution and at certain contact times. Therefore, it is possible that desorption occurs to a certain extent affecting net retention. In the case of desorption, the displaced H^+ ions are readsorbed to the clay and Fe oxide surfaces (Farrah & Pickering, 1978).

Hydrous oxide surfaces are normally covered with –OH groups that can act as powerful ligands for both soft and hard metal ions (Stumm et al., 1976). The distance between Fe oxides correlates well with the coordination polyhedra of most metal ions (Knox et al., 2000). The main functional group present on the bauxite surface is a hydroxyl group with minor functional groups such as carbonyl groups of carboxylic acids and alcohols, and oxides (Ghosh & Mishra, 2017). It has been proposed that metal sorption occurs usually on sorption sites by releasing H^+ ions (typically one or two per cation adsorbed) from kaolinite, goethite, and other oxide surfaces (Forbes et al., 1976; Kinniburgh & Jackson, 1982; Zang et al., 1994; Spark et al., 1995). The proton release from kaolinite usually happens at the edge sites (Spark et al., 1995). Even though the H^+ ions located at the outer hydroxyl plane are not readily exchangeable as those on broken edges, certain metals like Pb^{2+} could be adsorbed to those sites as well (Frost, 1998; Ma & Eggleton, 1999), suggesting selective adsorption. Studies have suggested unhydrolyzed adsorption (Barrow et al., 1981; Müller & Sigg, 1992), and unhydrolyzed and hydrolyzed adsorption (Forbes et al., 1976; Gunneriusson et al., 1994) especially during sorption on Fe oxyhydroxides.

Heavy metals are usually considered to be specifically adsorbing cations (Abd-Elfattah & Wada, 1981). The stability of coordination complexes formed via deprotonated COOH or OH groups tends to be higher than that of the ion-exchange complexes of hydrated metals (Abd-Elfattah & Wada, 1981). Compared to weakly adsorbing cations, strongly adsorbing ions have the ability to efficiently compete with protons for oxygen atoms in OH and COOH groups or water molecules. Therefore, the main mechanism of metal ion sorption should be through specific adsorption where the ions are adsorbed in the inner layer via oxygen atoms and hydroxyl groups. Other studies have also found that the positively charged surfaces on Al-Fe oxides and hydroxides particularly have the ability to adsorb heavy metals forming inner-sphere bonds (Bruemmer et al., 1988; Güçlü & Apak, 2003; Santona et al., 2006; Garau et al., 2007). However, metal ions, especially in cases where they show moderate affinities, can form ion-exchange complexes depending on the nature of the ion and their steric relationships (Abd-Elfattah & Wada, 1981).

Depending on the substrate, adsorption could be either through bidentate complexation (Bargar et al., 1997b) or monodentate complexation (Apak et al., 1998). Bargar et al. (1997a) found that metals can be preferentially adsorbed to edges of FeO or AlO octahedra. In their study, they suggest that bidentate complexation is preferred especially on goethite and hematite because the stabilization energy resulted by forming multiple bonds outweighs the destabilization caused by possible Fe-Pb repulsions at the edges of FeO octahedra. However, monodentate complexation occurs on AlO octahedra. They point out the reason for this difference could be the steric match of Pb trigonal pyramids with FeOH octahedra compared to AlO octahedra. Even though Fe and Al oxides share similar basic crystal chemistries and bulk

structures, and possibly form structurally similar metal sorption products, there could still be slight differences in the binding approaches.

The Freundlich isotherm model better describes heterogeneous surfaces, where the absorption sites are non-specific and non-uniform, while the Langmuir model assumes homogeneous distribution of binding sites on the sorbent surface and no interaction between molecules bound (Genç-Fuhrman et al., 2007; Saeedi et al., 2013). In general, our data better resemble the Langmuir isotherm model. However, it should be stressed that the isotherm fitting was simply an effort to identify if there is any correlation between the data set and these standard models. The number of data points was not sufficient to perform a standard isotherm analysis accurately. The higher correlation coefficient values obtained are most likely because of the lack of data points in curve fitting (even so, overall, they are slightly higher for Langmuir fitting). However, the shape of an isotherm is helpful in determining whether the sorption is favorable or unfavorable. The distribution of data points exhibits Langmuir-type behavior. The model parameters cannot be confidently used for interpretations (e.g., kL and Q_{max} of the Langmuir model to interpret how favorable conditions are to form sorbent-sorbate complexes, and obtain the maximum adsorption capacities, respectively). Generally, these parameters, especially Q_{max} values obtained, were slightly higher for Cu^{2+} (and Pb^{2+}) indicating higher affinity to bauxite. Based on the observed patterns, and calculated parameters (even with the errors associated) we can say that the Langmuir model fits better but not that data completely disagree with the Freundlich model. Studies report adsorption fitting both Langmuir and Freundlich models (Adebowale et al., 2005; Adebowale et al., 2006; Baral et al., 2007) and the modified Langmuir-Freundlich model works well for heterogeneous substrates which satisfy assumptions in both models. Fitting both models indicates chemisorptive mono-layer formation where the adsorption

process is predominantly chemical, but the sites are non-specific and non-uniform. According to these definitions, here the sorption sites are naturally both monolayer and hetero layer. This suggests the presence of various types of sorption sites and the possibility of them having different energies in case the sites were located on edges or in a defect position (Gupta & Bhattacharyya, 2008; Malamis & Katsou, 2013). Considering the physical and chemical (compositional) nature of bauxite, such indications seem to be in accord with its expected sorption mechanism, where chemisorption is dominant (not the only reaction) and heterogeneity plays a role in the process as well. The values of the Freundlich heterogeneity factor (n) in the range <1, 1-2, 2-10 indicate poor, moderate, and good adsorption characteristics, respectively (Wang et al., 2008; Lavecchia et al., 2012). Most of the obtained values in our study suggest moderate to good adsorption (Ni^{2+} is excluded due to negative data points). Studies have reported that sorption data fits the Langmuir model better at low concentrations in water but the Freundlich model at higher concentrations (Adebowale et al., 2006). This suggests the presence of certain sites responsible for metal ion adsorption and they result in monolayer coverage on the surface. As the sorbate concentration increases, more than one type of active sites may be involved in the sorption process (Adebowale et al., 2006). Genç-Fuhrman et al. (2004) noticed the ability of surface impurities to hinder the adsorption capacity of Bauxol (sea water-neutralized red mud). Cengeloglu et al. (2006) also made similar observations (monolayer adsorption) in their study on red mud (bauxite residue). Especially at low concentrations, when the driving force from the solution onto the substrate is low, only certain mineral assemblages on bauxite could be significant in the removal process. Here, the less heterogeneous mineral assemblages on heterogeneous surfaces result in a homogeneous surface of adsorption (Genç-Fuhrman et al., 2004; Cengeloglu et al., 2006). This also suggests the possibility of different

mineral species contributing to metal retention probably at varying significance as the conditions of the system change, which may lead to multiple sorption processes. If multiple sorption processes are involved (e.g., precipitation) besides adsorption, isotherm models may not be able to predict the removal process very well (Genç-Fuhrman et al., 2007).

5.2. The Effect of Sorbate Concentration on the Removal Process

Percent adsorption (fraction of metal ions adsorbed) decreases while uptake in general increases with increase in sorbate concentration. Similar observations have been made in other studies that tested various sorbent-heavy metal systems (Yu et al., 2000; Adebowale et al., 2005; Baral et al., 2007; Vieira et al., 2010; Ghosh & Mishra, 2017; Atasoy & Bilgic, 2018; Ouyang et al., 2019; Mu'azu et al., 2020). The decrease in percent adsorption or removal efficiency could be due to decrease in the active sites on the sorbents as more sorbates are adsorbed. At low metal concentrations, the amount of active adsorption sites should be available in excess thus the adsorption could be independent of the metal concentration. At fixed sorbent dose, the number of active sites is unchanged but the number of ions to accommodate increases creating a competitive environment reducing overall removal efficiency (Adebowale et al., 2005; Bhattacharyya & Gupta, 2008b; Vieira et al., 2010). Sorption is favorable at higher initial metal concentrations because of the increasing driving force of the metal ions towards the active sorption sites. The higher probability of interaction between sorbent and sorbate increases the adsorption capacity (Adebowale et al., 2005; Mu'azu et al., 2020).

5.3. The Effect of Contact Time on the Removal Process

Studies show that the metal adsorption on sorbents increases for a certain period of contact time, and remains constant (Gupta & Sharma 2002; Genç et al., 2003; Jiang et al., 2010; Nadaroglu et al., 2010; Ghosh & Mishra, 2017; Atasoy & Bilgic, 2018). This could be a result of adsorbed ion aggregating or blocking access to internal pores (Bouhamed et al., 2014). Even though the active adsorption sites on the sorbent decrease interacting with metal ions, the sorption rate depends on the sorbates transported from the liquid phases to actual adsorption sites, resulting in increase in removal until saturation (Yu et al., 2000; Duan et al., 2016). However, in our study, it was not common to see metals reaching a defined plateau. Some of the samples showed a decrease in adsorption after the peak adsorption while some of them showed variation in adsorption with contact time attaining higher percent adsorptions more than once. It is difficult to give a direct explanation for the scenario of significant fluctuations within the same series. The attainment of equilibrium depends on the sorbate, sorbent, and their interactions (Gupta & Bhattacharyya, 2008). Ouyang et al. (2019) observed two equilibrium stages (stagnant removal percentages) in their study on heavy metal- synthetic porous material (composed of bauxite, silicate tailings, bentonite, $Fe_2(SO_4)_3$, $MgSO_4$, and $Na(HCO_3)$ systems. The first stage of equilibrium could be due to the adsorption saturation of the outer surface as it is in direct contact with the solution. Metal ion permeation into the pores could take time and the second equilibrium indicates the saturation of the inner surface of the pores. Researchers have reported situations where sorption hardly attains a clear equilibrium within the selected time periods making it difficult to determine the optimum adsorption densities (McConchie et al., 1999; Genç-Fuhrman et al., 2005). Also, some studies report that contact time has a negligible effect, especially at higher sorbate concentrations, suggesting immediate adsorption (Baral et al., 2007).

At 500 ppb, as clearly shown by Pb^{2+} and Co^{2+}, the systems show a tendency to attain an equilibrium stage, but at lower concentrations, the fluctuations in uptake with contact time seem to be unpredictable. Therefore, it was difficult to observe a dependency of sorption on contact time. Proton transfer at the surface can change the chemical conditions with time (e.g., influence the charge of the substrate). Also, even though we carried the experiment without controlling pH in order to have less control over the natural reactions, the solution pH can change as the reactions proceed. The stabilization pH could differ resulting in fluctuations in uptake. Occurrence of various rate processes with time controls the kinetics of the interactions. It is usually expected that the initial higher rate of adsorption decreases as more metals start to cover the adsorption sites, thus the rate is gradually becoming dependent on the rate at which the ions are transported from the bulk phases to the sorbent-sorbate interface (Yu et al., 2000; Gupta & Bhattacharyya, 2008). However, due to the observed behavior in uptake and inability to find consistent experimental equilibrium concentrations, interpreting data using kinetic models with confidence is not feasible.

5.4. Selective Sorption by Bauxite

Bauxite is not equally efficient in removing all the metal ions. Overall, Cu^{2+} and Pb^{2+} have higher affinities to bauxite. Cu^{2+}, in particular, shows some of the highest available percent adsorption values, suggesting near-complete removal of the ion from solution. Usually, the ionic radius and the valence of cations influence relative selectivity in solution, but the behavior of heavy metal ions could be complex than this manner (Puls & Bohn, 1988; Saha et al., 2001). Studies that used either Pb^{2+} or Cu^{2+} individually in their experiments often reported that these metals showed the highest affinities toward the sorbent (Zang et al., 1994; Singh et al., 2001;

Klauber et al., 2011; Atasoy & Bilgic, 2018; Mu'azu et al., 2020). Examples of sorbents used in these studies are phosphatic clay, bauxite, gypsum amended bauxite residue, montmorillonite, and goethite. Even acid soils that contain species such as humus, Fe-oxides, allophene, and halloysite can strongly adsorb Pb^{2+} and Cu^{2+} (Abd-Elfattah & Wada, 1981). Atasoy & Bilgic (2018) reports maximum Cu^{2+} values of 99.65% on bauxite that are comparable to our data. Similar to our study, Co^{2+} and Ni^{2+} are often ranked lower than Pb^{2+} and Cu^{2+} in terms of removal efficiency or adsorption capacity (Grimme, 1968; Forbes et al., 1976; Abd-Elfattah & Wada, 1981; Klauber et al., 2011; Mu'azu et al., 2020). When used together, most studies rank Cu^{2+} higher than Pb^{2+} (Grimme, 1968; Forbes et al., 1976; Kinniburgh et al., 1976). However, some studies, which particularly focused on clays such as kaolin or kaolinite, rank Pb^{2+} higher than Cu^{2+} in terms of removal capacity of the sorbent (Adebowale et al., 2005; Jiang et al., 2010) while substrates such as goethite and Al gel prefer Cu^{2+} over Pb^{2+}. Therefore, kaolinite (clays) may favor Pb^{2+}, while goethite and oxides may favor Cu^{2+}. Being a composite of these mineral phases, our bauxite samples showed higher affinities towards both of these metals and the values of removal efficiency and uptake of these metals were not drastically different from each other. Pb^{2+} removal efficiencies by B2 especially at higher sorbate concentrations are higher compared to those by B1, and this difference is clear in multi-metal-bauxite systems. B2 is rich in kaolinite, which suggests that kaolinite influences sorption and its selectivity towards Pb^{2+}. However, overall, Cu^{2+} which is more likely to be preferred by goethite and oxides shows higher removal very often. This indicates that Fe oxyhydroxides could host the adsorption sites that are mainly responsible for adsorption.

Electronegativity and hydrated ionic radius of divalent metal ions can contribute to adsorption. A smaller hydrated ionic radius allows the ion to move closer to the sorbent surface

and also to easily enter the channels in the substrate for preferential adsorption (Minceva et al., 2007; Loganathan et al., 2018). Ions with low hydration energy can be easily dehydrated and shrink for better adsorption. The (generally) observed sequence of removal (Cu^{2+}>Pb^{2+}> $Co^{2+}$and Ni^{2+}) does not correlate with the order of ionic radii (Pb 1.20A, Cu-Ni-Co around 0.72A) or the Pauling electronegativity (Pb 2.33, Cu 1.9, Ni 1.91, and Co 1.88). It has been suggested that the hydrolysis properties of the metals show a correlation to the adsorption pattern (Forbes et al., 1976; Kinniburgh et al., 1976; Adebowale et al., 2005; Klauber et al., 2011). The higher hydrolysis constants of Pb (7.8-7.9) and Cu (7.3-8.0) indicate that these metals are readily hydrolyzed (Sillén & Martell, 1965; Abd-Elfattah & Wada, 1981). However, the dependence of Cu^{2+} on the surface charge is comparatively small and the planes of the H^{+} and adsorbed Cu^{2+} are significantly closer. This distance is higher for other ions such as Pb^{2+} and Co^{2+} (Forbes et al., 1976). Hence, the effect of the surface coverage on the adsorption energy is lowest for Cu^{2+} showing the highest affinity for the substrate. Even if Cu^{2+} and Pb^{2+} have similar affinities, Pb^{2+} should have very high interaction energy due to its large radius (Pb 1.271, Cu 0.728). Also, according to the Irving-Williams order of divalent metal ions, Cu^{2+} has the highest stability constant of the formed complex regardless of the nature of the ligand (Apak et al., 1998).

Ni^{2+} at certain concentrations and contact times shows a contrasting behavior to other ions suggesting release of Ni^{2+}, not adsorption. Ni^{2+} shows certain similarities to the adsorption pattern by Co^{2+}, which is quite different from Pb^{2+} and Cu^{2+}. However, Co^{2+} did not show any negative adsorption percentages. Compared to metals such as Cu^{2+}, Ni^{2+} has a higher tendency to associate with easily reducible and exchangeable phases which may lead to higher chance of releasing from the substrate (Saeedi et al., 2013). Therefore, it is possible that some ions may be released to water during the adsorption process (Genç et al., 2003), but the current data are not

sufficient to give a conclusion on this matter. Additional analyses, especially on bauxite composition, need to be done to further discuss this observation.

5.5. The Effect of the Presence of Multiple Metal Ions in Solution on the Removal Process

Metal ions often coexist in water (wastewater in particular). Generally, the removal efficiencies of the single-element experiments were higher than those of ME-experiments. Different ions competing for the available adsorption sites result in a strong competition among metals, interfering with each other hence suppressing sorption and decreasing the individual removal (Loganathan et al., 2018; Ouyang et al., 2019).

CHAPTER 6 - CONCLUSION AND SUGGESTIONS FOR FUTURE WORK

Raw bauxite exhibits promising properties as a low-cost adsorbent to remove heavy metals from polluted water. The metal retention ability could be attributed to Fe-Al-Ti oxyhyroxides, clay minerals, and the organic matter content in the samples. Fe-oxyhydroxides and kaolinite are supposedly the major hosts for binding sites. Multiple reactions could be contributing to the sorption of metal ions onto bauxite. The main mechanism of metal sorption occurs via inner sphere complexation where the metals adsorb through –OH bridges releasing protons. Ion-exchange reactions may occur especially on clays contributing to metal ion retention. Even though the differences are not significant, adsorption follows the Langmuir isotherm model better than the Freundlich model, indicating chemisorptive mono-layer formation. Isotherm data suggest that one mineral assemblage is specifically responsible for adsorption, thus this species in heterogeneous bauxite acts as a homogeneous surface, especially at lower sorbate concentrations. However, the nature of adsorption could change as the conditions in the system change and at higher concentrations.

In general, the adsorption capacity of bauxite increases but, the removal efficiency decreases with increase in metal ion concentration in water. Sample B1 (goethite-rich bauxite) shows a slightly higher dependency on the initial metal concentration in solution. Overall, sample B2 (kaolinite-rich bauxite) has a higher removal efficiency. Sorption does not have a significant relationship with the contact time. It is expected that at higher sorbate concentrations, the removal process will become more or less independent of the contact time. Both types of

bauxite preferably adsorbed Cu^{2+} and Pb^{2+}, and are generally specifically selective towards Cu^{2+}. Even though the Co^{2+} and Ni^{2+} seem to have similar affinities toward bauxite, further analysis is needed to confirm the behavior of Ni^{2+}. Coexisting metal ions result in a competitive environment and interfere with the sorption mechanisms, reducing the overall removal of metal ions in solution. Therefore, the type of bauxite, initial metal concentration in water, type of metal, and interference by mutually existing metal ions all influence ion adsorption to bauxite. Multiple experiments with each different variable are recommended to test this hypothesis further. Also, a detailed kinetic study, and a leaching experiment to test possible desorption would be beneficial in the future.

REFERENCES

Ageena, N. A. (2010). The use of local sawdust as an adsorbent for the removal of copper Ion from wastewater using fixed bed adsorption. Engineering and Technology Journal, 28(2).

Abd-Elfattah, A., & Wada, K. (1981). Adsorption of lead, copper, zinc, cobalt, and cadmium by soils that differ in cation-exchange materials. Journal of Soil Science, 32(2). https://doi.org/10.1111/j.1365-2389.1981.tb01706.x

Adebowale, K. O., Unuabonah, I. E., & Olu-Owolabi, B. I. (2005). Adsorption of some heavy metal ions on sulfate- and phosphate-modified kaolin. Applied Clay Science, 29(2). https://doi.org/10.1016/j.clay.2004.10.003

Adebowale, K. O., Unuabonah, I. E., & Olu-Owolabi, B. I. (2006). The effect of some operating variables on the adsorption of lead and cadmium ions on kaolinite clay. Journal of Hazardous Materials, 134(1–3). https://doi.org/10.1016/j.jhazmat.2005.10.056

Ali, I., & Gupta, V. K. (2007). Advances in water treatment by adsorption technology. Nature Protocols, 1(6). https://doi.org/10.1038/nprot.2006.370

Alshaebi, F. Y., Yaacob, W. Z., Samsudin, A. R., & Alsabahi, E. (2009). Arsenic Adsorption on Bauxite Mineral Using Batch Equilibrium Test. American Journal of Applied Sciences, 6(10). https://doi.org/10.3844/ajassp.2009.1826.1830

Altundoğan, H. S., Altundoğan, S., Tümen, F., & Bildik, M. (2002). Arsenic adsorption from aqueous solutions by activated red mud. Waste Management, 22(3). https://doi.org/10.1016/S0956-053X(01)00041-1

Apak, R., Güçlü, K., & Turgut, M. H. (1998). Modeling of copper(II), cadmium(II), and lead(II) adsorption on red mud. Journal of Colloid and Interface Science, 203(1). https://doi.org/10.1006/jcis.1998.5457

Atasoy, A. D., & Bilgic, B. (2018). Adsorption of Copper and Zinc Ions from Aqueous Solutions Using Montmorillonite and Bauxite as Low-Cost Adsorbents. Mine Water and the Environment, 37(1). https://doi.org/10.1007/s10230-017-0464-2

Aziz, H. A., Adlan, M. N., & Ariffin, K. S. (2008). Heavy metals (Cd, Pb, Zn, Ni, Cu and Cr(III)) removal from water in Malaysia: Post treatment by high quality limestone. Bioresource Technology, 99(6). https://doi.org/10.1016/j.biortech.2007.04.007

Balan, E., Allard, T., Boizot, B., Morin, G., & Muller, J. P. (1999). Structural Fe3+ in natural kaolinites: new insights from electron paramagnetic resonance spectra fitting at X and Q-band frequencies. Clays and clay minerals, 47(5), 605-616.

Baral, S. S., Das, S. N., Rath, P., & Chaudhury, G. R. (2007). Chromium(VI) removal by calcined bauxite. Biochemical Engineering Journal, 34(1). https://doi.org/10.1016/j.bej.2006.11.019

Bargar, J. R., Brown Jr, G. E., & Parks, G. A. (1997a). Surface complexation of Pb (II) at oxide-water interfaces: I. XAFS and bond-valence determination of mononuclear and polynuclear Pb (II) sorption products on aluminum oxides. Geochimica et Cosmochimica Acta, 61(13), 2617-2637.

Bargar, J. R., Brown, G. E., & Parks, G. A. (1997b). Surface complexation of Pb(II) at oxide-water interfaces: II. XAFS and bond-valence determination of mononuclear Pb(II) sorption products and surface functional groups on iron oxides. Geochimica et Cosmochimica Acta, 61(13). https://doi.org/10.1016/S0016-7037(97)00125-7

Barrow, N. J., Bowden, J. W., Posner, A. M., & Quirkw, J. P. (1981). Describing the adsorption of copper, zinc and lead on a variable charge mineral surface. Australian Journal of Soil Research, 19(3). https://doi.org/10.1071/SR9810309

Bereket, G., Aroğuz, A. Z., & Özel, M. Z. (1997). Removal of Pb(II), Cd(II), Cu(II), and Zn(II) from aqueous solutions by adsorption on bentonite. Journal of Colloid and Interface Science, 187(2). https://doi.org/10.1006/jcis.1996.4537

Bermond, A., & Bourgeois, S. (1992). Influence of soluble organic matter on cadmium mobility in model compounds and in soils. The Analyst, 117 3. https://doi.org/10.1039/an9921700685

Bhattacharyya, K. G., & Gupta, S. sen. (2008a). Adsorption of a few heavy metals on natural and modified kaolinite and montmorillonite: A review. In Advances in Colloid and Interface Science (Vol. 140, Issue 2). https://doi.org/10.1016/j.cis.2007.12.008

Bhattacharyya, K. G., & Gupta, S. sen. (2008b). Kaolinite and montmorillonite as adsorbents for Fe(III), Co(II) and Ni(II) in aqueous medium. Applied Clay Science, 41(1–2). https://doi.org/10.1016/j.clay.2007.09.005

Bicker Jr, A.R. (1969). Geologic map of Mississippi: Mississippi Geological Survey.

Boily, J. F., & Fein, J. B. (1996). Experimental study of cadmium-citrate co-adsorption onto α-Al2O3. Geochimica et Cosmochimica Acta, 60(16). https://doi.org/10.1016/0016-7037(96)00131-7

Bouhamed, F., Elouear, Z., Bouzid, J., & Ouddane, B. (2014). Batch sorption of Pb(II) ions from aqueous solutions using activated carbon prepared from date stones: Equilibrium, kinetic, and thermodynamic studies. Desalination and Water Treatment, 52(10–12). https://doi.org/10.1080/19443994.2013.806222

Bruemmer, G. W., Gerth, J., & Tiller, K. G. (1988). Reaction kinetics of the adsorption and desorption of nickel, zinc and cadmium by goethite. I. Adsorption and diffusion of

metals. Journal of Soil Science, 39(1). https://doi.org/10.1111/j.1365-2389.1988.tb01192.x

Brunori, C., Cremisini, C., Massanisso, P., Pinto, V., & Torricelli, L. (2005). Reuse of a treated red mud bauxite waste: Studies on environmental compatibility. Journal of Hazardous Materials, 117(1). https://doi.org/10.1016/j.jhazmat.2004.09.010

Buechakd, E. F. (1925). Bauxite in Northeastern Mississippi.

Burchard, E. F. (1924). Bauxite associated with siderite. Bulletin of the Geological Society of America, 35(3). https://doi.org/10.1130/GSAB-35-437

Cengeloglu, Y., Tor, A., Ersoz, M., & Arslan, G. (2006). Removal of nitrate from aqueous solution by using red mud. Separation and Purification Technology, 51(3). https://doi.org/10.1016/j.seppur.2006.02.020

Cherukumilli, K., Delaire, C., Amrose, S., & Gadgil, A. J. (2017). Factors Governing the Performance of Bauxite for Fluoride Remediation of Groundwater. Environmental Science and Technology, 51(4). https://doi.org/10.1021/acs.est.6b04601

Conant, L. C. (1949). Bauxite and kaolin deposits of Mississippi, exclusive of the Tippah-Benton district. Geological Survey Bulletin, (1199), 1.

Das, N., Pattanaik, P., & Das, R. (2005). Defluoridation of drinking water using activated titanium rich bauxite. Journal of Colloid and Interface Science, 292(1). https://doi.org/10.1016/j.jcis.2005.06.045

Davis, J. A., & Leckie, J. O. (1978). Surface ionization and complexation at the oxide/water interface II. Surface properties of amorphous iron oxyhydroxide and adsorption of metal ions. Journal of Colloid and Interface Science, 67(1). https://doi.org/10.1016/0021-9797(78)90217-5

Duan, P., Yan, C., Zhou, W., & Ren, D. (2016). Development of fly ash and iron ore tailing based porous geopolymer for removal of Cu(II) from wastewater. Ceramics International, 42(12). https://doi.org/10.1016/j.ceramint.2016.05.143

Duplantis, M. J. (1975). Depositional Systems in the Midway and Wilcox Groups: Paleocene-Lower Eocene, North Mississippi (Doctoral dissertation, University of Mississippi).

Farrah, H., & Pickering, W. F. (1978). Extraction of heavy metal ions sorbed on clays. Water, Air, and Soil Pollution, 9(4). https://doi.org/10.1007/BF00213544

Forbes, E. A., Posner, A. M., & Quirk, J. P. (1976). The specific adsorption of divalent Cd, Co, Cu, Pb, and Zn on goethite. Journal of Soil Science, 27(2). https://doi.org/10.1111/j.1365-2389.1976.tb01986.x

Friesl, W., Friedl, J., Platzer, K., Horak, O., & Gerzabek, M. H. (2006). Remediation of contaminated agricultural soils near a former Pb/Zn smelter in Austria: Batch, pot and

field experiments. Environmental Pollution, 144(1). https://doi.org/10.1016/j.envpol.2006.01.012

Frost, R. L. (1998). Hydroxyl deformation in kaolins. Clays and Clay Minerals, 46(3). https://doi.org/10.1346/CCMN.1998.0460307

Fuge, R., Pearce, F. M., Pearce, N. J. G., & Perkins, W. T. (1993). Geochemistry of Cd in the secondary environment near abandoned metalliferous mines, Wales. Applied Geochemistry, 8. https://doi.org/10.1016/S0883-2927(09)80006-1

Garau, G., Castaldi, P., Santona, L., Deiana, P., & Melis, P. (2007). Influence of red mud, zeolite and lime on heavy metal immobilization, culturable heterotrophic microbial populations and enzyme activities in a contaminated soil. Geoderma, 142(1–2). https://doi.org/10.1016/j.geoderma.2007.07.011

Genç, H., Tjell, J. C., McConchie, D., & Schuiling, O. (2003). Adsorption of arsenate from water using neutralized red mud. Journal of Colloid and Interface Science, 264(2). https://doi.org/10.1016/S0021-9797(03)00447-8

Genç-Fuhrman, H., Bregnhøj, H., & McConchie, D. (2005). Arsenate removal from water using sand-red mud columns. Water Research, 39(13). https://doi.org/10.1016/j.watres.2005.04.050

Genç-Fuhrman, H., Mikkelsen, P. S., & Ledin, A. (2007). Simultaneous removal of As, Cd, Cr, Cu, Ni and Zn from stormwater: Experimental comparison of 11 different sorbents. Water Research, 41(3). https://doi.org/10.1016/j.watres.2006.10.024

Genç-Fuhrman, H., Tjell, J. C., & McConchie, D. (2004). Increasing the arsenate adsorption capacity of neutralized red mud (Bauxsol). Journal of Colloid and Interface Science, 271(2). https://doi.org/10.1016/j.jcis.2003.10.011

Ghosh, D., & Bhattacharyya, K. G. (2002). Adsorption of methylene blue on kaolinite. Applied Clay Science, 20(6). https://doi.org/10.1016/S0169-1317(01)00081-3

Ghosh, M. R., & Mishra, S. P. (2017). Effect of Co-ions on Cr(VI) and F - Adsorption by Thermally Treated Bauxite (TTB). Arabian Journal for Science and Engineering, 42(10). https://doi.org/10.1007/s13369-017-2472-8

Grim, R. E. (1962). Applied clay mineralogy.

Grim, R. E. (1968). Clay mineralogy.

Grimme, H. (1968). Adsorption of Mn, Co, Cu and Zn by goethite from dilute solutions. Journal of Plant Nutrition and Soil Science, 121, 58-65.

Güçlü, K., & Apak, R. (2003). Modeling the adsorption of free and heavy metal complex-bound EDTA onto red mud by a nonelectrostatic surface complexation model. Journal of Colloid and Interface Science, 260(2). https://doi.org/10.1016/S0021-9797(03)00045-6

Gunneriusson, L., Lövgren, L., & Sjöberg, S. (1994). Complexation of Pb(II) at the goethite (α-FeOOH)/water interface: The influence of chloride. Geochimica et Cosmochimica Acta, 58(22). https://doi.org/10.1016/0016-7037(94)90225-9

Gupta, S. sen., & Bhattacharyya, K. G. (2008). Immobilization of Pb(II), Cd(II) and Ni(II) ions on kaolinite and montmorillonite surfaces from aqueous medium. Journal of Environmental Management, 87(1). https://doi.org/10.1016/j.jenvman.2007.01.048

Gupta, V. K., & Sharma, S. (2002). Removal of cadmium and zinc from aqueous solutions using red mud. Environmental Science and Technology, 36(16). https://doi.org/10.1021/es020010v

Halim, M., Conte, P., & Piccolo, A. (2003). Potential availability of heavy metals to phytoextraction from contaminated soils induced by exogenous humic substances. Chemosphere, 52(1). https://doi.org/10.1016/S0045-6535(03)00185-1

Hedrich, S., & Johnson, D. B. (2014). Remediation and selective recovery of metals from acidic mine waters using novel modular bioreactors. Environmental Science and Technology, 48(20). https://doi.org/10.1021/es5030367

Hind, A. R., Bhargava, S. K., & Grocott, S. C. (1999). The surface chemistry of Bayer process solids: A review. In Colloids and Surfaces A: Physicochemical and Engineering Aspects (Vol. 146, Issues 1–3). https://doi.org/10.1016/S0927-7757(98)00798-5

Huang, W., Wang, S., Zhu, Z., Li, L., Yao, X., Rudolph, V., & Haghseresht, F. (2008). Phosphate removal from wastewater using red mud. Journal of Hazardous Materials, 158(1). https://doi.org/10.1016/j.jhazmat.2008.01.061

Jiang, M. qin, Jin, X. ying, Lu, X. Q., & Chen, Z. liang. (2010). Adsorption of Pb(II), Cd(II), Ni(II) and Cu(II) onto natural kaolinite clay. Desalination, 252(1–3). https://doi.org/10.1016/j.desal.2009.11.005

Kinniburgh, D. G., & Jackson, M. L. (1982). Concentration and pH Dependence of Calcium and Zinc Adsorption by Iron Hydrous Oxide Gel. Soil Science Society of America Journal, 46(1). https://doi.org/10.2136/sssaj1982.03615995004600010010x

Kinniburgh, D. G., Jackson, M. L., & Syers, J. K. (1976). Adsorption of Alkaline Earth, Transition, and Heavy Metal Cations by Hydrous Oxide Gels of Iron and Aluminum. Soil Science Society of America Journal, 40(5). https://doi.org/10.2136/sssaj1976.03615995004000050055x

Klauber, C., Gräfe, M., & Power, G. (2011). Bauxite residue issues: II. options for residue utilization. Hydrometallurgy, 108(1–2). https://doi.org/10.1016/j.hydromet.2011.02.007

Knox, A., Seaman, J., Mench, M., & Vangronsveld, J. (2000). Remediation of Metal- and Radionuclides-Contaminated Soils by In Situ Stabilization Techniques. In Environmental Restoration of Metals-Contaminated Soils. https://doi.org/10.1201/9781420026269.ch2

Lane, H. C. (1973). Soil Survey, Pontotoc County, Mississippi. US Department of Agriculture, Soil Conservation Service.

Lavecchia, R., Medici, F., Piga, L., Rinaldi, G., & Zuorro, A. (2012). Fluoride removal from water by adsorption on a high alumina content bauxite. Chemical Engineering Transactions, 26. https://doi.org/10.3303/CET1226038

Lee, A. Y. W., Lim, S. F., Chua, S. N. D., Sanaullah, K., Baini, R., & Abdullah, M. O. (2017). Adsorption Equilibrium for Heavy Metal Divalent Ions (Cu2+, Zn2+, and Cd2+) into Zirconium-Based Ferromagnetic Sorbent. Advances in Materials Science and Engineering, 2017. https://doi.org/10.1155/2017/1210673

Lehmann, M., Zouboulis, A. I., & Matis, K. A. (1999). Removal of metal ions from dilute aqueous solutions: A comparative study of inorganic sorbent materials. Chemosphere, 39(6). https://doi.org/10.1016/S0045-6535(99)00031-4

Liu, Y., Naidu, R., & Ming, H. (2011). Red mud as an amendment for pollutants in solid and liquid phases. In Geoderma (Vol. 163, Issues 1–2). https://doi.org/10.1016/j.geoderma.2011.04.002

Loganathan, P., Shim, W. G., Sounthararajah, D. P., Kalaruban, M., Nur, T., & Vigneswaran, S. (2018). Modelling equilibrium adsorption of single, binary, and ternary combinations of Cu, Pb, and Zn onto granular activated carbon. Environmental Science and Pollution Research, 25(17). https://doi.org/10.1007/s11356-018-1793-9

López, E., Soto, B., Arias, M., Núñez, A., Rubinos, D., & Barral, M. T. (1998). Adsorbent properties of red mud and its use for wastewater treatment. Water Research, 32(4). https://doi.org/10.1016/S0043-1354(97)00326-6

Ma, C., & Eggleton, R. A. (1999). Cation exchange capacity of kaolinite. Clays and Clay Minerals, 47(2). https://doi.org/10.1346/ccmn.1999.0470207

Malakootian, M., Javdan, M., & Iranmanesh, F. (2014). Fluoride Removal from Aqueous Solutions Using Bauxite Activated Mines in Yazd Province (Case Study: Kuhbanan Water). Journal of Community Hearth Research, 3(2).

Malamis, S., & Katsou, E. (2013). A review on zinc and nickel adsorption on natural and modified zeolite, bentonite and vermiculite: Examination of process parameters, kinetics and isotherms. In Journal of Hazardous Materials (Vols. 252–253). https://doi.org/10.1016/j.jhazmat.2013.03.024

Manning, B. A., & Goldberg, S. (1996). Modeling arsenate competitive adsorption on kaolinite, montmorillonite and illite. Clays and Clay Minerals, 44(5). https://doi.org/10.1346/CCMN.1996.0440504

McConchie, D., Clark, M., Hanahan, C., & Fawkes, R. (1999). The use of seawater-neutralised bauxite refinery residues (red mud) in environmental remediation programs. Proceedings of the TMS Fall Extraction and Processing Conference, 1.

Mellen, F. F. (1939) Winston County mineral resources: Mississippi State Geological Survey Bulletin. 38, pp 169.

Minceva, M., Markovska, L., & Meshko, V. (2007). Removal of Zn2+, Cd2+ and Pb2+ from binary aqueous solution by natural zeolite and granulated activated carbon. In Macedonian Journal of Chemistry and Chemical Engineering (Vol. 26, Issue 2).

Morse, P. F. (1923) The bauxite deposits Mississippi Geological Survey Bulletin. 19, p. 1-208.

Mu'azu, N. D., Bukhari, A., & Munef, K. (2020). Effect of montmorillonite content in natural Saudi Arabian clay on its adsorptive performance for single aqueous uptake of Cu(II) and Ni(II). Journal of King Saud University - Science, 32(1). https://doi.org/10.1016/j.jksus.2018.06.003

Müller, B., & Sigg, L. (1992). Adsorption of lead(II) on the goethite surface: Voltammetric evaluation of surface complexation parameters. Journal of Colloid and Interface Science, 148(2). https://doi.org/10.1016/0021-9797(92)90187-Q

Nadaroglu, H., Kalkan, E., & Demir, N. (2010). Removal of copper from aqueous solution using red mud. Desalination, 251(1–3). https://doi.org/10.1016/j.desal.2009.09.138

Ouyang, D., Zhuo, Y., Hu, L., Zeng, Q., Hu, Y., & He, Z. (2019). Research on the adsorption behavior of heavy metal ions by porous material prepared with silicate tailings. Minerals, 9(5). https://doi.org/10.3390/min9050291

Pandya, D. N. (1973). A Study of the Bauxitic Deposits Along the Midway-Wilcox Contact in Oktibbeha County, Mississippi (Doctoral dissertation, Mississippi State University).

Parfitt, R. L., Giltrap, D. J., & Whitton, J. S. (1995). Contribution of organic matter and clay minerals to the cation exchange capacity of soils. Communications in Soil Science and Plant Analysis, 26(9–10). https://doi.org/10.1080/00103629509369376

Petrović, M., Kaštelan-Macan, M., & Horvat, A. J. M. (1999). Interactive sorption of metal ions and humic acids onto mineral particles. Water, Air, and Soil Pollution, 111(1–4). https://doi.org/10.1023/a:1005084802830

Priddy. R.R. (1943). Pontotoc County Mineral Resources: Mississippi Geological Survey Bulletin 54, pp. 16-25.

Puls, R. W., & Bohn, H. L. (1988). Sorption of Cadmium, Nickel, and Zinc by Kaolinite and Montmorillonite Suspensions. Soil Science Society of America Journal, 52(5). https://doi.org/10.2136/sssaj1988.03615995005200050013x

Rao, R. A. K., Ikram, S., & Uddin, M. K. (2014). Removal of Cd(II) from aqueous solution by exploring the biosorption characteristics of gaozaban (Onosma bracteatum). Journal of Environmental Chemical Engineering, 2(2). https://doi.org/10.1016/j.jece.2014.04.008

Rao, R. A. K., & Kashifuddin, M. (2014). Kinetics and isotherm studies of Cd(II) adsorption from aqueous solution utilizing seeds of bottlebrush plant (Callistemon chisholmii). Applied Water Science, 4(4). https://doi.org/10.1007/s13201-014-0153-2

Reed, D. F. (1952). Investigation of High-alumina Clays and Bauxite of Northeastern Mississippi (Vol. 4827). US Department of the Interior, Bureau of Mines.

Rodda, D. P., Wells, J. D., & Johnson, B. B. (1996). Anomalous adsorption of copper(II) on goethite. Journal of Colloid and Interface Science, 184(2). https://doi.org/10.1006/jcis.1996.0652

Russell, J. D., Parfitt, R. L., Fraser, A. R., & Farmer, V. C. (1974). Surface structures of gibbsite goethite and phosphated goethite. Nature, 248(5445). https://doi.org/10.1038/248220a0

Saadi, Z., Saadi, R., & Fazaeli, R. (2013). Fixed-bed adsorption dynamics of Pb (II) adsorption from aqueous solution using nanostructured γ-alumina. Journal of Nanostructure in Chemistry, 3(1). https://doi.org/10.1186/2193-8865-3-48

Saeedi, M., Li, L. Y., Karbassi, A. R., & Zanjani, A. J. (2013). Sorbed metals fractionation and risk assessment of release in river sediment and particulate matter. Environmental Monitoring and Assessment, 185(2). https://doi.org/10.1007/s10661-012-2664-3

Saha, U. K., Taniguchi, S., & Sakurai, K. (2001). Adsorption Behavior of Cadmium, Zinc, and Lead on Hydroxyaluminum- and Hydroxyaluminosilicate-Montmorillonite Complexes. Soil Science Society of America Journal, 65(3). https://doi.org/10.2136/sssaj2001.653694x

Santona, L., Castaldi, P., & Melis, P. (2006). Evaluation of the interaction mechanisms between red muds and heavy metals. Journal of Hazardous Materials, 136(2). https://doi.org/10.1016/j.jhazmat.2005.12.022

Sillén, L. G., & Martell, A. E. (1965). Stability Constants of Metallic-ion Complexes. Soil Science, 100(1). https://doi.org/10.1097/00010694-196507000-00026

Silva, F. A. N. G., Medeiros, M. E., Sampaio, J. A., Santos, R. D., Carneiro, M. C., Costa, L. S., & Garrido, F. M. S. (2009). Technological characterization of bauxite from Pará-Brazil. TMS Light Metals.

Singh, S. P., Ma, L. Q., & Harris, W. G. (2001). Heavy Metal Interactions with Phosphatic Clay: Sorption and Desorption Behavior. Journal of Environmental Quality, 30(6). https://doi.org/10.2134/jeq2001.1961

Soares, M. R., & Alleoni, L. R. F. (2008). Contribution of soil organic carbon to the ion exchange capacity of tropical soils. Journal of Sustainable Agriculture, 32(3). https://doi.org/10.1080/10440040802257348

Spark, K. M., Johnson, B. B., & Wells, J. D. (1995). Characterizing heavy-metal adsorption on oxides and oxyhydroxides. European Journal of Soil Science, 46(4). https://doi.org/10.1111/j.1365-2389.1995.tb01358.x

Stumm, W., Dalang, F., & Hohl, H. (1976). Interaction of Metal Ions with Hydrous Oxide Surfaces. Croatica Chemica Acta, 48(4).

Tanabe, K. (1981). Solid Acid and Base Catalyst in Catalysis Science and Technology. by Anderson, JR, Boudart, M., Springer, Berlin, 2, 233.

Thompson, C. N. (1980). Petrology of North Mississippi bauxite: a case for depositional bauxite and kaolin (M.S. thesis, University of Mississippi).

Tschapek, M., Tcheichvili, L., & Wasowski, C. (1974). The point of zero charge (pzc) of kaolinite and SiO2+AI2O3 mixtures. Clay Minerals, 10(4). https://doi.org/10.1180/claymin.1974.010.4.01

Uddin, M. K. (2017). A review on the adsorption of heavy metals by clay minerals, with special focus on the past decade. In Chemical Engineering Journal (Vol. 308). https://doi.org/10.1016/j.cej.2016.09.029

Vieira, M. G. A., Neto, A. F. A., Gimenes, M. L., & da Silva, M. G. C. (2010). Sorption kinetics and equilibrium for the removal of nickel ions from aqueous phase on calcined Bofe bentonite clay. Journal of Hazardous Materials, 177(1–3). https://doi.org/10.1016/j.jhazmat.2009.12.040

Wang, Y. H., Lan, Y., & Huang, C. B. (2008). Adsorption behavior of Pb2+ and Cd2+ ions on bauxite flotation tailings. Journal of Central South University of Technology (English Edition), 15(2). https://doi.org/10.1007/s11771-008-0035-6

Weber Jr, W. J. (1985). Adsorption theory, concepts and models. Adsorption technology: a step-by-step approach to process evaluation and application, 1-35.

Williamson, D. R. (1976). Investigation of the Tertiary lignites of Mississippi (No. MGS-74-1). Mississippi Geological Survey, Jackson (USA).

Yabe, M. J. S., & de Oliveira, E. (2003). Heavy metals removal in industrial effluents by sequential adsorbent treatment. Advances in Environmental Research, 7(2). https://doi.org/10.1016/S1093-0191(01)00128-9

Yong, R. N., Mohamed, A. M. O., & Warkentin, B. P. (1992). Contaminant soil interaction. Principles of Contaminant Transport in Soils. Elsevier, Amsterdam, Holland, 143-180.

Yu, B., Zhang, Y., Shukla, A., Shukla, S. S., & Dorris, K. L. (2000). The removal of heavy metal from aqueous solutions by sawdust adsorption - Removal of copper. Journal of Hazardous Materials, 80(1–3). https://doi.org/10.1016/S0304-3894(00)00278-8

Zang, L., Liu, C. Y., & Ren, X. M. (1994). Adsorption of cations on TiO2 particles. A method to determine the surface density of OH groups. Journal of the Chemical Society, Chemical Communications, 16. https://doi.org/10.1039/C39940001865

LIST OF APPENDICES

APPENDIX A: ADSORPTION ISOTHERMS

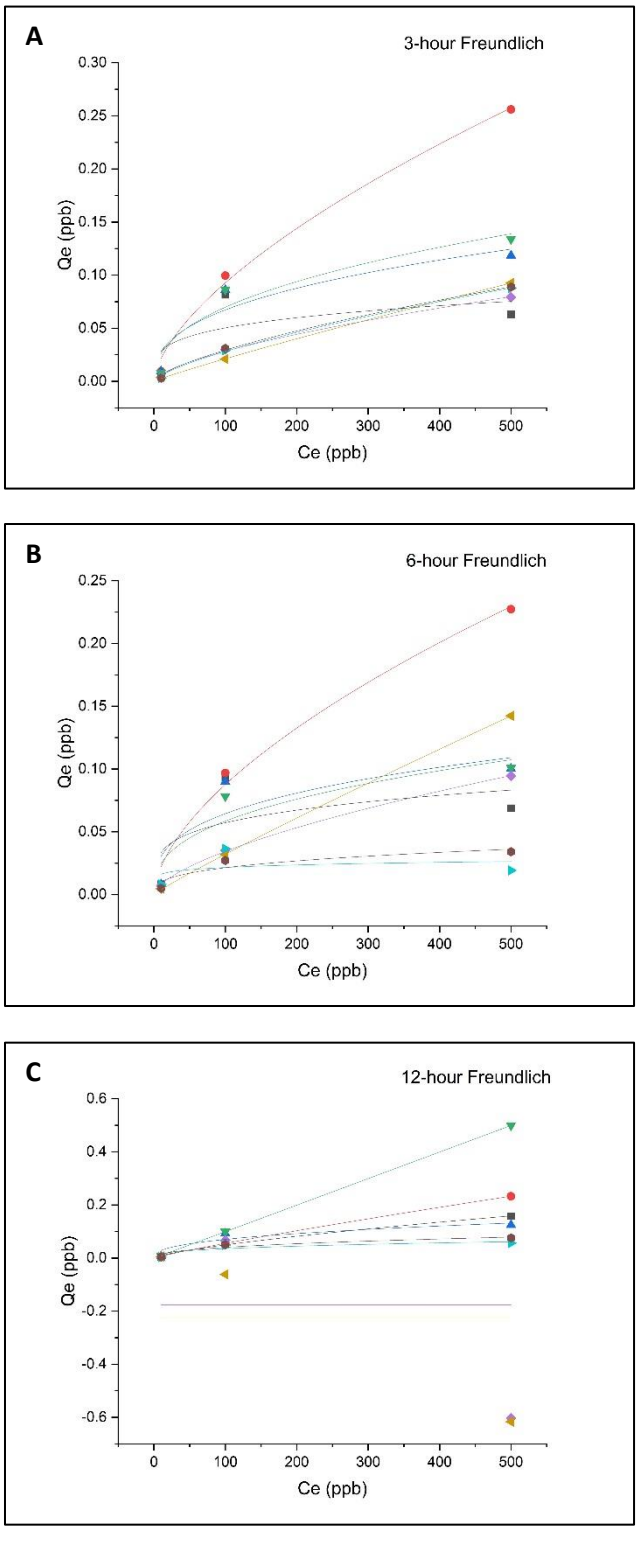

Figure (continued)

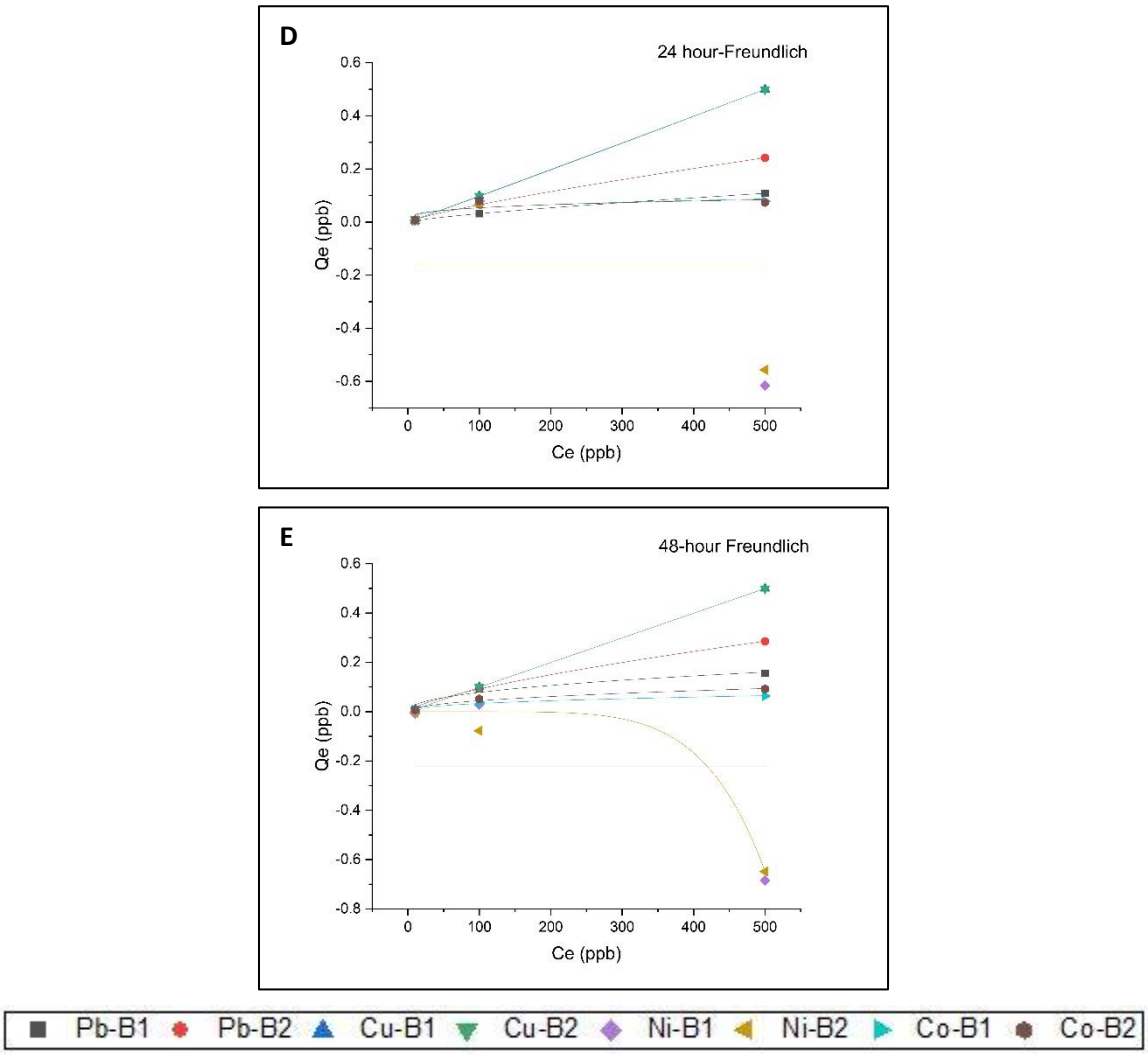

Figure 16. Freundlich isotherms (non-linear method) obtained for the adsorption of Pb^{2+}, Cu^{2+}, Ni^{2+}, and Co^{2+} in single-element solutions onto bauxite (B1 and B2) at different contact periods. A) 3 hours. B) 6 hours. C) 12 hours. D) 24 hours. E) 48 hours.

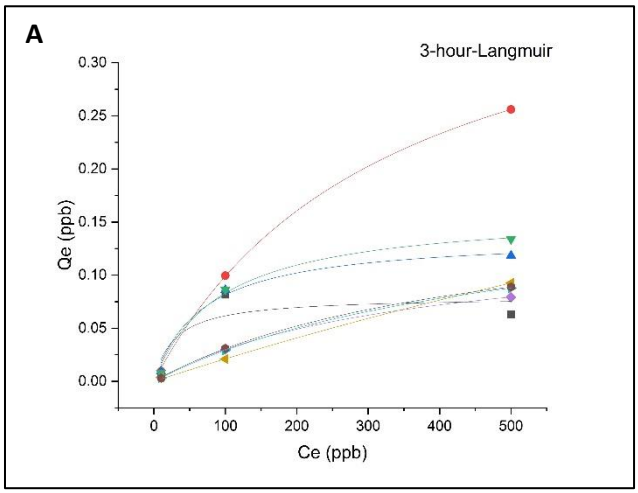

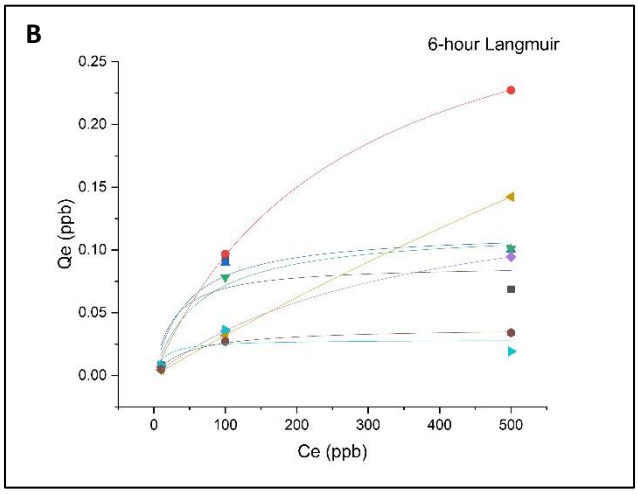

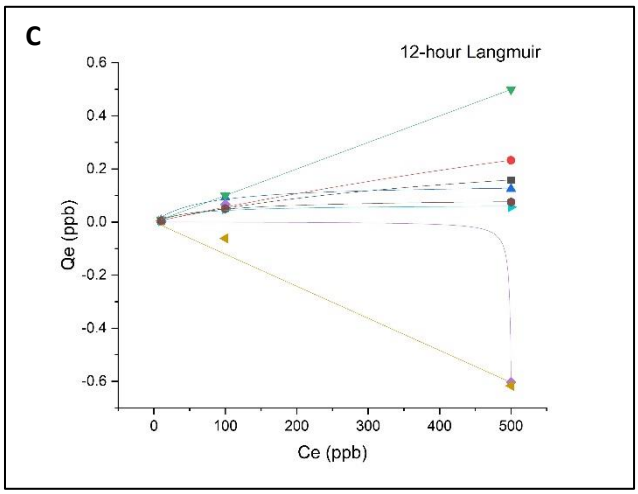

Figure (continued)

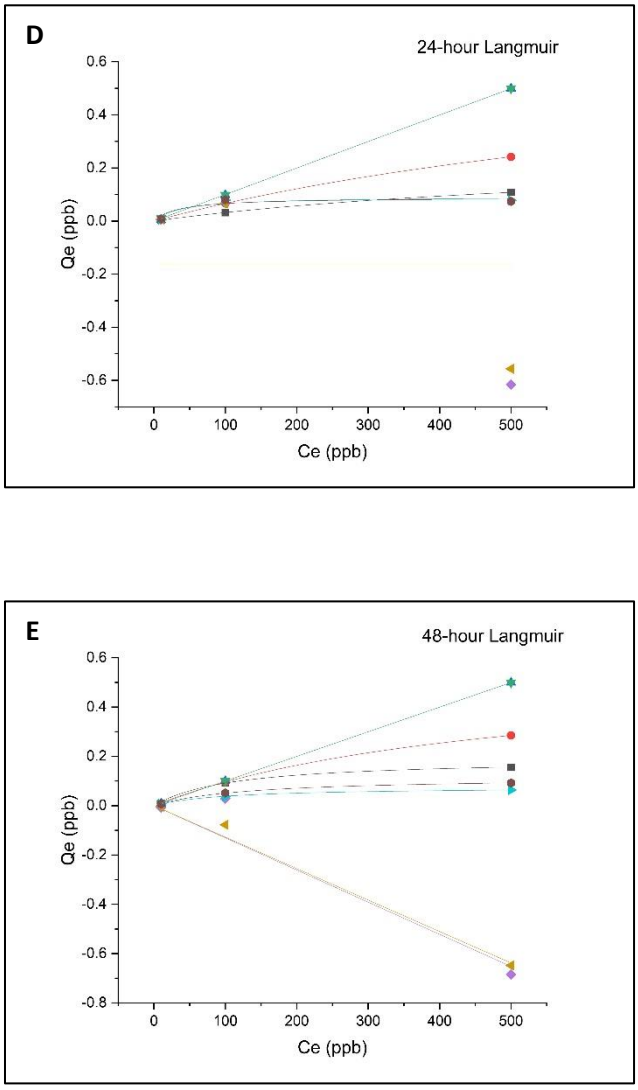

Figure 17. Langmuir isotherms (non-linear method) obtained for the adsorption of Pb^{2+}, Cu^{2+}, Ni^{2+}, and Co^{2+} in single-element solutions onto bauxite (B1 and B2) at different contact periods. A) 3 hours. B) 6 hours. C) 12 hours. D) 24 hours. E) 48 hours.

APPENDIX B: TABLES

Table 1. Final metal concentrations (ppb) in the B1-single-metal systems

B1					
Initial Concentration	Time \ Cation	Pb^{2+}	Cu^{2+}	Ni^{2+}	Co^{2+}
10	3	4.495	0.594872	6.557741	6.739799
	6	1.767782	1.95515	3.316764	1.93011
	12	4.990904	3.566483	4.099791	6.998369
	24	5.534858	5.594502	5.140559	4.974489
	48	0.805404	0.5	17.67952	2.896786
100	3	18.44	13.99855	69.90737	70.7107
	6	7.012228	10.0439	64.76893	63.61655
	12	48.41434	7.738018	33.56205	50.77909
	24	68.16063	1.734515	32.44879	21.37793
	48	5.962796	0.5	71	61.93838
500	3	437	381.5535	420.6703	412.1787
	6	431.2848	399.8325	405.4064	480.8031
	12	341.7705	375.3351	1102.838	443.4336
	24	392.1302	0.5	1115.795	422.2357
	48	344.5711	0.5	1184.303	436.7191

The values in the shaded cells are inferred based on the respective minimum detection limits. The hollow points on the graphs correspond to these values.

Table 2. Final metal concentrations (ppb) in the B2-single-metal systems

B2					
Initial Concentration	Time \ Cation	Pb^{2+}	Cu^{2+}	Ni^{2+}	Co^{2+}
10	3	0.458	2.066954	6.339799	6.887512
	6	2.984986	4.796738	5.324309	4.928815
	12	6.311195	0.5	4.705	5.500603
	24	3.694303	0.13574	3.871916	2.21497
	48	0.845468	0.5	13.71886	3.249843
100	3	0.458	13.6157	79.00763	69.09587
	6	3.114956	21.70176	68.12338	72.87494
	12	43.56429	0.5	161.6911	49.31339
	24	33.53238	1.850416	33.96417	19.99028
	48	3.793745	0.5	177.8075	48.76637
500	3	244	366.0205	407.4055	411.1378
	6	272.636	399.0339	357.6356	465.9459
	12	267.112	0.5	1116.377	424.421
	24	258.278	0.5	1056.537	425.8418
	48	215.2004	0.5	1148.134	407.9467

The values in the shaded cells are inferred based on the respective minimum detection limits. The hollow points on the graphs correspond to these values.

Table 3. Final metal concentrations (ppb) in the B1-multi-element (ME) systems

ME B1					
Initial Concentration	Time \ Cation	Pb^{2+}	Cu^{2+}	Ni^{2+}	Co^{2+}
10	3	0.458	0.5	7.8	6.7
	6	0.458	3.79	7.4	4.12
	12	8.85	13.8	4.775	7.2
	24	8.876636	4.866279	4.171363	3.244771
	48	0.458	2.805	7.45	5.8
100	3	61.4	82.6	89	92
	6	102.8	106.4	87.2	96.2
	12	53	27.8	40.4	53.6
	24	65.2334	3.010134	34.31338	20.25329
	48	64.4	78.4	82.6	87.2
500	3	498	437	434	451
	6	519	501	438	486
	12	481	416	406	444
	24	504	434	424	440
	48	511	467	425	470

The values in the shaded cells are inferred based on the respective minimum detection limits. The hollow points on the graphs correspond to these values.

Table 4. Final metal concentrations (ppb) in the B2-multi-element (ME) systems

ME B2					
Initial Concentration	Cation / Time	Pb^{2+}	Cu^{2+}	Ni^{2+}	Co^{2+}
10	3	0.458	3.6	8.3	9.15
	6	0.458	5.8	8.45	9.6
	12	5.5	5.7	5.85	6
	24	2.647505	3.690732	4.016181	2.083626
	48	0.458	2.645	7.5	6.4
100	3	46.8	72.6	83.2	87.4
	6	47.4	97.6	82.8	95
	12	46.8	100.8	41	54
	24	45.31524	33.32057	38.29166	20.217
	48	40.6	69.2	85.8	84.4
500	3	433	419	436	451
	6	486	440	454	450
	12	715	474	425	455
	24	454	499	437	458
	48	450	464	412	450

The values in the shaded cells are inferred based on the respective minimum detection limits. The hollow points on the graphs correspond to these values.

Table 5. Percentage adsorption by B1 treated with the single-element solutions

% adsorption B1					
Initial Concentration	Time / Cation	Pb^{2+}	Cu^{2+}	Ni^{2+}	Co^{2+}
10	3	55.05	94.051281	34.42259	32.602
	6	82.32218	80.448501	66.83236	80.6989
	12	50.09096	64.335167	59.00209	30.0163
	24	44.65142	44.054981	48.59441	50.2551
	48	91.94596	95	-76.7952	71.0321
100	3	81.56	86.001449	30.09263	29.2893
	6	92.98777	89.956105	35.23107	36.3835
	12	51.58566	92.261982	66.43795	49.2209
	24	31.83937	98.265485	67.55121	78.6221
	48	94.0372	99.5	29	38.0616
500	3	12.6	23.6893	15.86594	17.5643
	6	13.74304	20.033498	18.91872	3.83938
	12	31.6459	24.932983	-120.568	11.3133
	24	21.57395	99.9	-123.159	15.5529
	48	31.08578	99.9	-136.861	12.6562

Table 6. Percentage adsorption by B2 treated with the single-element solutions

% adsorption B2					
Initial Concentration	Time / Cation	Pb^{2+}	Cu^{2+}	Ni^{2+}	Co^{2+}
10	3	95.42	79.33046	36.60201	31.12488
	6	70.15014	52.03262	46.75691	50.71185
	12	36.88805	95	52.95	44.99397
	24	63.05697	98.6426	61.28084	77.8503
	48	91.54532	95	-37.1886	67.50157
100	3	95.42	86.3843	20.99237	30.90413
	6	96.88504	78.29824	31.87662	27.12506
	12	56.43571	99.5	-61.6911	50.68661
	24	66.46762	98.14958	66.03583	80.00972
	48	96.20625	99.5	-77.8075	51.23363
500	3	51.2	26.7959	18.5189	17.77244
	6	45.47279	20.19322	28.47289	6.810819
	12	46.5776	99.9	-123.275	15.11581
	24	48.3444	99.9	-111.307	14.83165
	48	56.95991	99.9	-129.627	18.41066

Table 7. Percentage adsorption by B1 treated with the multi-element solutions

%adsorption MEB1					
Initial Concentration	Time / Cation	Pb^{2+}	Cu^{2+}	Ni^{2+}	Co^{2+}
10	3	95.42	95	22	33
	6	95.42	62.1	26	58.8
	12	11.5	-	52.25	28
	24	11.23364	51.337206	58.28637	67.5523
	48	95.42	71.95	25.5	42
100	3	38.6	17.4	11	8
	6	-	-	12.8	3.8
	12	47	72.2	59.6	46.4
	24	34.7666	96.989866	65.68662	79.7467
	48	35.6	21.6	17.4	12.8
500	3	0.4	12.6	13.2	9.8
	6	-	-	12.4	2.8
	12	3.8	16.8	18.8	11.2
	24	-	13.2	15.2	12
	48	-	6.6	15	6

Table 8. Percentage adsorption by B2 treated with the multi-element solutions

%adsorption MEB2					
Initial Concentration	Time \ Cation	Pb^{2+}	Cu^{2+}	Ni^{2+}	Co^{2+}
10	3	95.42	64	17	8.5
	6	95.42	42	15.5	4
	12	45	43	41.5	40
	24	73.52495	63.09268	59.83819	79.16374
	48	95.42	73.55	25	36
100	3	53.2	27.4	16.8	12.6
	6	52.6	2.4	17.2	5
	12	53.2	-	59	46
	24	54.68476	66.67943	61.70834	79.783
	48	59.4	30.8	14.2	15.6
500	3	13.4	16.2	12.8	9.8
	6	2.8	12	9.2	10
	12	-	5.2	15	9
	24	9.2	0.2	12.6	8.4
	48	10	7.2	17.6	10

Table 9. Uptake by B1 treated with the single-element solutions

Qe B1					
Initial Concentration	Time \ Cation	Pb^{2+}	Cu^{2+}	Ni^{2+}	Co^{2+}
10	3	0.005505	0.009405	0.003442	0.00326
	6	0.008232	0.008045	0.006683	0.00807
	12	0.005009	0.006434	0.0059	0.003002
	24	0.004465	0.004405	0.004859	0.005026
	48	0.009195	0.0095	-0.00768	0.007103
100	3	0.08156	0.086001	0.030093	0.029289
	6	0.092988	0.089956	0.035231	0.036383
	12	0.051586	0.092262	0.066438	0.049221
	24	0.031839	0.098265	0.067551	0.078622
	48	0.094037	0.0995	0.029	0.038062
500	3	0.063	0.118447	0.07933	0.087821
	6	0.068715	0.100167	0.094594	0.019197
	12	0.158229	0.124665	-0.60284	0.056566
	24	0.10787	0.4995	-0.6158	0.077764
	48	0.155429	0.4995	-0.6843	0.063281

Table 10. Uptake by B2 treated with the single-element solutions

Qe B2					
Initial Concentration	Time \ Cation	Pb^{2+}	Cu^{2+}	Ni^{2+}	Co^{2+}
10	3	0.009542	0.007933	0.00366	0.003112
	6	0.007015	0.005203	0.004676	0.005071
	12	0.003689	0.0095	0.005295	0.004499
	24	0.006306	0.009864	0.006128	0.007785
	48	0.009155	0.0095	-0.00372	0.00675
100	3	0.099542	0.086384	0.020992	0.030904
	6	0.096885	0.078298	0.031877	0.027125
	12	0.056436	0.0995	-0.06169	0.050687
	24	0.066468	0.09815	0.066036	0.08001
	48	0.096206	0.0995	-0.07781	0.051234
500	3	0.256	0.13398	0.092594	0.088862
	6	0.227364	0.100966	0.142364	0.034054
	12	0.232888	0.4995	-0.61638	0.075579
	24	0.241722	0.4995	-0.55654	0.074158
	48	0.2848	0.4995	-0.64813	0.092053

Table 11. Uptake by B1 treated with the multi-element solutions

Qe MEB1					
Initial Concentration	Time \ Cation	Pb^{2+}	Cu^{2+}	Ni^{2+}	Co^{2+}
10	3	0.009542	0.0095	0.0022	0.0033
	6	0.009542	0.00621	0.0026	0.00588
	12	0.00115	-0.0038	0.005225	0.0028
	24	0.001123	0.005134	0.005829	0.006755
	48	0.009542	0.007195	0.00255	0.0042
100	3	0.0386	0.0174	0.011	0.008
	6	-0.0028	-0.0064	0.0128	0.0038
	12	0.047	0.0722	0.0596	0.0464
	24	0.034767	0.09699	0.065687	0.079747
	48	0.0356	0.0216	0.0174	0.0128
500	3	0.002	0.063	0.066	0.049
	6	-0.019	-0.001	0.062	0.014
	12	0.019	0.084	0.094	0.056
	24	-0.004	0.066	0.076	0.06
	48	-0.011	0.033	0.075	0.03

Table 12. Uptake by B2 treated with the multi-element solutions

Qe MEB2					
Initial Concentration	Time \ Cation	Pb^{2+}	Cu^{2+}	Ni^{2+}	Co^{2+}
10	3	0.009542	0.0064	0.0017	0.00085
	6	0.009542	0.0042	0.00155	0.0004
	12	0.0045	0.0043	0.00415	0.004
	24	0.007352	0.006309	0.005984	0.007916
	48	0.009542	0.007355	0.0025	0.0036
100	3	0.0532	0.0274	0.0168	0.0126
	6	0.0526	0.0024	0.0172	0.005
	12	0.0532	-0.0008	0.059	0.046
	24	0.054685	0.066679	0.061708	0.079783
	48	0.0594	0.0308	0.0142	0.0156
500	3	0.067	0.081	0.064	0.049
	6	0.014	0.06	0.046	0.05
	12	-0.215	0.026	0.075	0.045
	24	0.046	0.001	0.063	0.042
	48	0.05	0.036	0.088	0.05

Table 13. Langmuir model parameters for B1-single-metal systems

Sample	Pb B1			Cu B1			Ni B1			Co B1		
Time \ Parameter	Qmax	Kl	R2	Qmax	Kl	R2	Qmax	Kl	R2	Qmax	Kl	R2
3 hr	0.07964	0.03436	0.7564	0.13677	0.0147	0.98549	0.13457	0.00287	0.99997	0.1758	0.002	0.99999
6 hr	0.08803	0.03773	0.73194	0.11533	0.02195	F 0.93976	0.161	0.00284	0.99872	0.02846	0.07356	0.46748
12 hr	0.32921	0.00185	0.99992	0.1451	0.01441	0.97436	0.00238	-0.00199	F 0.98348	0.06547	0.01965	0.93938
24 hr	0.26521	0.00137	0.99986	696.02	1.44E-06	F 0.93976	-0.18112	-4.75E+43	-5.6E-10	0.09164	0.02521	0.88781
48hr	0.18996	0.00927	F 0.99484	323.889	3.09E-06	F 1	-31215.4	4.18E-08	F 0.91793	0.07576	0.01013	0.99999

Table 14. Langmuir model parameters for B2-single-metal systems

Sample	Pb B2			Cu B2			Ni B2			Co B2		
Time \ Parameter	Qmax	Kl	R2	Qmax	Kl	R2	Qmax	Kl	R2	Qmax	Kl	R2
3 hr	0.42464	0.00304	0.9997	0.16021	0.01077	0.99128	0.58817	3.74E-04	0.99951	0.1681	0.00224	0.99991
6 hr	0.34732	0.0038	F 0.99861	0.11695	0.01585	0.9664	1.01857	3.25E-04	0.99982	0.03798	0.02127	F 0.98989
12 hr	1.09426	5.41E-04	F 0.99983	286.7532	3.49E-06	F 1	-8104.28	1.49E-07	F 0.98304	0.08938	0.0118	F 0.98989
24 hr	0.71323	0.00103	0.99997	553.3392	1.81E-06	F 0.99998	-0.16146	3.33E+44	-1.93E-10	0.08802	0.02967	0.8687
48hr	0.56185	0.00206	0.99988	327.8101	3.05E-06	F 1	-11427.8	1.12E-07	F 0.98929	0.11593	0.00777	0.9992

Table 15. Freundlich model parameters for B1-single-metal systems

Sample	Pb B1			Cu B1			Ni B1			Co B1		
Time / Parameter	KF	n	R2	KF	n	R2	KF	n	R2	KF	n	R2
3 hr	0.01592	3.99918	0.4768	0.01159	2.61863	0.88374	0.00148	1.55972	0.99586	0.00109	1.4139	0.9983
6 hr	0.01955	4.29059	0.44171	0.01429	3.05818	0.75924	0.0019	1.58946	0.99934	0.01215	8.03461	0.17267
12 hr	0.00178	1.38368	0.99811	0.01166	2.56436	0.86273	-0.17683	-1.76E+20	-2.22E-16	0.00714	2.88949	0.77124
24 hr	9.23E-04	1.30525	F 0.99982	8.95E-04	0.98256	F 0.99982	-0.18113	-4.63E+24	F 2.22045E	0.01297	3.26599	F 0.66799
48hr	0.00991	2.23424	0.94175	9.80E-04	0.99694	F 1	-0.22099	-1.44E+20	0	0.00478	2.3846	9.64E-01

Table 16. Freundlich model parameters for B2-single-metal systems

Sample	Pb B2			Cu B2			Ni B2			Co B2		
Time / Parameter	KF	n	R2	KF	n	R2	KF	n	R2	KF	n	R2
3 hr	0.005	1.58E+00	0.99383	0.00977	2.34099	0.92243	3.18719E-4	1.09582	0.99973	0.00124	1.45277	0.99719
6 hr	0.00557	1.67163	0.98705	0.01032	2.6534	0.83893	4.54E-04	1.08124	0.99993	0.00477	3.07069	0.86352
12 hr	9.07E-04	1.11993	0.99956	9.80E-04	0.99694	1	-0.22426	-1.17E+26	-2.22E-16	0.00598	2.41065	0.90855
24 hr	0.00152	1.22607	F 0.99949	9.36E-04	0.98956	1	-0.16146	-9.05E+18	1.11E-16	0.01492	3.59485	0.62393
48hr	0.00358	1.41904	0.99748	9.80E-04	0.99694	F 1	-2.62E-17	0.16463	9.76E-01	0.00515	2.13978	0.9666

VITA

Hashindra Herath was born and raised in Matale, Sri Lanka. She graduated from the Govt. Science College (high school), Matale and entered the University of Peradeniya, Sri Lanka to earn her Bachelor of Science. Graduated with a special degree in Geology, she went on to work as a teaching assistant in the same university and then as a geologist at the National Building Research Organization during the next 1 ½ year. Following her passion for the research in the field of geoscience, in 2018, Hashindra joined the University of Mississippi. She worked as a teaching assistant during her stay in the Department of Geology and Geological Engineering. She is graduating in 2021 with a Master of Science and was also the recipient of the Dawn Blackledge Scholarship (2020) and the Outstanding Graduate Student (MS) in Geology and Geological Engineering Award (2021). After graduation, Hashindra is starting her PhD at the University of Arkansas.